THE UNIVERSITY of EDINBURGH

Edinburgh Research Explorer

Phycobiliproteins from extreme environments and their potential applications

Citation for published version:
Puzorjov, A & McCormick, A 2020, 'Phycobiliproteins from extreme environments and their potential applications', *Journal of Experimental Botany*. https://doi.org/10.1093/jxb/eraa139

Digital Object Identifier (DOI):
10.1093/jxb/eraa139

Link:
Link to publication record in Edinburgh Research Explorer

Document Version:
Peer reviewed version

Published In:
Journal of Experimental Botany

Publisher Rights Statement:
This is a pre-copyedited, author-produced version of an article accepted for publication in Journal of Experimental Botany following peer review. The version of record Anton Puzorjov, Alistair J McCormick, Phycobiliproteins from extreme environments and their potential applications, Journal of Experimental Botany, , eraa139, 10.1093/jxb/eraa139 is available online at: https://doi.org/10.1093/jxb/eraa139

General rights
Copyright for the publications made accessible via the Edinburgh Research Explorer is retained by the author(s) and / or other copyright owners and it is a condition of accessing these publications that users recognise and abide by the legal requirements associated with these rights.

Take down policy
The University of Edinburgh has made every reasonable effort to ensure that Edinburgh Research Explorer content complies with UK legislation. If you believe that the public display of this file breaches copyright please contact openaccess@ed.ac.uk providing details, and we will remove access to the work immediately and investigate your claim.

OPEN ACCESS

Download date: 09. May. 2024

Phycobiliproteins from extreme environments and their potential applications

Anton Puzorjov, Alistair J. McCormick[†]

SynthSys and Institute of Molecular Plant Sciences, School of Biological Sciences, University of Edinburgh, Edinburgh, EH9 3BF, UK.

[†]corresponding author:
Dr Alistair J. McCormick
Daniel Rutherford Building
SynthSys and Institute of Molecular Plant Sciences
School of Biological Sciences
University of Edinburgh
The King's Buildings
EH9 3BF
Phone: +44 (0)1316505316
Email: alistair.mccormick@ed.ac.uk

Additional details

	ORCID	ResearcherID
Alistair J. McCormick	0000-0002-7255-872X	B-1558-2008

Running title: Phycobiliproteins from extreme environments

Abstract: 139
Length: 6,658
Figures: 3
Tables: 2

Highlight: We review research on phycobilisomes from extremophile cyanobacteria and red algae and their structural stability adaptations, and we discuss the potential applications of phycobiliproteins from extremophiles for commercial applications.

Keywords: *Arthrospira platensis*, colourant, photosynthesis, phycobilisome, phycocyanin, *Synechococcus*, *Synechocystis*, *Thermosynechococcus*, thermophilic

Abbreviations: APC, allophycocyanin; PBP, phycobiliprotein; PBS, phycobilosome; PC, phycocyanin; PCB, phycocyanobilin; PE, phycoerythrin; PEB, phycoerythrobilin; PEC, phycoerythrocyanin; PSI, photosystem I; PSII, photosystem II; PUB, phycourobilin; PVB, phycoviolobilin.

Abstract

The light harvesting phycobilisome complex is an important component of photosynthesis in cyanobacteria and red algae. Phycobilisomes are composed of phycobiliproteins, including the blue phycobiliprotein phycocyanin, that are considered high value products with applications in several industries. Remarkably, several cyanobacteria and red algal species retain the capacity to harvest light and photosynthesise under highly selective environments such as hot springs and flourish in extremes of pH and elevated temperatures. These thermophilic organisms produce thermostable phycobiliproteins, which have superior qualities much needed for wider adoption of these natural pigment-proteins in the food, textile and other industries. Here we review the available literature on the thermostability of phycobilisome components from thermophilic species and discuss how a better appreciation of phycobiliproteins from extreme environments will benefit our fundamental understanding of photosynthetic adaptation and could provide a sustainable resource for several industrial processes.

Introduction

Phycobilisomes (PBSs) are large, light harvesting complexes that improve the efficiency of light capture in the visible spectrum and help to push the boundaries where phototrophic species can survive. PBSs are located on the outer surface of thylakoid membranes in prokaryotic cyanobacteria and some eukaryotic algae, such as the Rhodophyta (red algae) and Glaucophyta, and range in size from 3000 to 7000 kDa. PBSs funnel light energy that falls in the spectral gap between the major absorption bands of chlorophyll (500-660 nm) to the photosystem reaction centres of PSI and PSII. This is particularly advantageous in aquatic habitats, as longer wavelengths of visible light preferentially absorbed by chlorophyll (i.e. red light) penetrate less well through water than shorter wavelengths (i.e. green and blue light) (Samsonoff and MacColl, 2001; Adir, 2005; Blot et al., 2009). A secondary role for the PBS is nitrogen storage, as indicated by the rapid PBS degradation upon nitrogen starvation (Yamanaka and Glazer, 1980; Carrieri et al., 2017; Ruan et al., 2018). PBSs are found in microbes from a wide range of ecological niches including those that grow in extreme environments, such as high temperatures and acidic conditions. Remarkably, in those environments the components of PBSs have evolved relatively minor structural modifications that significantly enhance stability and preserve pigment-protein function even under conditions at the biological limits of phototrophic life.

The PBS complex is primarily made up of an array of coloured and highly fluorescent phycobiliproteins (PBPs) that are of commercial interest owing to a host of potentially useful properties (e.g. antioxidant, anti-inflammatory, antiplatelet, anti-cancer, antifungal and antiviral), and thus could have applications in several industries, including pharmaceuticals, nutraceuticals and cosmetics (Li et al., 2019; Kannaujiya et al., 2019; Pagels et al., 2019). Currently, PBPs are considered high value products for their pigment properties, in particular, the blue PBP phycocyanin (PC), which is a highly sought after natural colourant in the food and cosmetics industries (Kannaujiya et al., 2017). Nevertheless, the stability of PBPs remains a key issue for commercial applications. For example, PC is harvested primarily from the alkaliphilic cyanobacterium *Arthrospira platensis* (commonly known as Spirulina) (Sarada et al., 1999; Ogbonda et al., 2007; Pan-utai et al., 2018). Compared to synthetic blue dyes (e.g. Brilliant Blue FCF), PC from *A. platensis* is unstable and prone to discolouration outside of a relatively narrow range of temperature and pH conditions (Chaiklahan et al., 2012). Identifying alternative sources for stable PBPs, or genetically improving the stability properties of PBPs in mesophilic species would be highly desirable and could lead to an increase in commercial uptake (Dejsungkranont et al., 2017; Falkeborg et al., 2018; Böcker et al., 2019).

In this review, we first provide a brief overview of the component parts and assembly of PBSs. We then compare the performances of PBSs and PBPs obtained from hyperthermophilic, thermophilic and mesophilic organisms under high temperatures (with particular focus on the high value product PC) and discuss their structural adaptations. Finally, we discuss the current and potential commercial uses of PBPs and suggest industrial applications that could greatly benefit from the properties of PBPs from extremophile species.

Overview of phycobiliproteins structure and phycobilisome assembly

A typical PBP is composed of a stable heterodimer complex of an α- and β-subunit (an (αβ) monomer) to which one to three linear tetrapyrrole bilin chromophores are covalently bound at well-conserved cysteine residues on each subunit via thioether bonds (**Fig. 1A**). The chromophores assume rigid, extended conformations when attached (Zhao et al., 2006; Scheer and Zhao, 2008). Biosynthesis of all bilin chromophores starts with the non-proteinogenic amino acid δ-aminolevulinic acid, which is converted to cyclic heme in the tetrapyrrole biosynthesis pathway (Beale, 1994). Cyclic heme is cleaved by heme oxygenase

(HO) to yield linear biliverdin IX⍺ (BV) (**Fig. 1B**). BV is an ancient and common bilin chromophore used by phytochrome photoreceptors in bacteria and fungi (Lamparter, 2004). In cyanobacteria and eukaryotic photosynthetic organisms, BV is further reduced by a family of ferredoxin-dependent bilin reductases, which act to decrease the number of double bonds in the π conjugation system of the subsequent chromophore. This leads to a shift in the absorption peak typical for BV adducts (*ca*. 700 nm) towards lower wavelengths more suited for light capture in aquatic environments (Cornejo and Beale, 1988; Cornejo et al., 1998; Lamparter, 2004; Wagner et al., 2007).

Four types of bilin chromophores are found in cyanobacteria: phycocyanobilin (PCB), phycoerythrobilin (PEB), phycourobilin (PUB) and phycoviolobilin (PVB) (**Fig. 1B**) (Glazer, 1989). Phycocyanobilin:ferredoxin oxidoreductase (PcyA) catalyses the reduction of BV to PCB in a one-step reaction. In contrast, biosynthesis of PEB is typically a two-step reaction catalysed firstly by 15,16-dihydrobiliverdin:ferredoxin oxidoreductase (PebA), which reduces the C-15 methine bridge of BV to produce intermediate 15,16-dihydrobiliverdin (DHBV), and secondly by phycoerythrobilin:ferredoxin oxidoreductase (PebB), which reduces the A-ring diene structure of DHBV to produce PEB (Dammeyer and Frankenberg-Dinkel, 2006). The majority of PBPs in cyanobacteria and red algae require specific PBP lyases for covalent attachment of the bilin chromophores to conserved cysteine residues on their cognate apo-protein subunits, with the exception of the allophycocyanin core linker (ApcE) that can autocatalytically bind to PCB (for review see Scheer and Zhao, 2008). In addition to chromophore attachment, the heterodimeric lyase-isomerase, PecE/PecF, also converts PCB into the Δ4-to-Δ2 double bond isomer PVB (Zhao et al., 2000). Similarly, the lyase-isomerase, RpcG, converts PEB into the Δ4-to-Δ2 double bond isomer PUB (Blot et al., 2009).

The classification of PBPs is based on the type and number of bilin chromophores they bind. There are three classes of PBPs: (1) allophycocyanin (APC) containing a total of two PCB chromophores with the major absorption peak at 650 nm, (2) phycocyanin (PC) containing three PCB chromophores with the major absorption peak at 620 nm and phycoerythrocyanin (PEC) containing two PCB chromophores and one PVB chromophore with the major absorption peak at 570 nm (Zhao et al., 2003) and (3) four subclasses of phycoerythrin (PE) containing a total of five or six PUB and PEB chromophores with two absorption peaks at *ca*. 495 and 560 nm, respectively (Glazer, 1984; MacColl et al., 1996; Alvey et al., 2011;

Vásquez-Suárez et al., 2018). A prefix can be added before the PBP class to indicate specific spectral properties of the attached chromophore(s) (e.g. C-PC and R-PC) (De Marsac, 2003; Six et al., 2007; Kumar et al., 2016).

The assembly of PBPs into a mature PBS complex is a multi-step process. Initially, three ($\alpha\beta$) monomers combine to form a trimeric $(\alpha\beta)_3$ disk, then two $(\alpha\beta)_3$ trimers can aggregate to form a dual-disk $(\alpha\beta)_6$ hexamer. Subsequently, the disks are stacked and linked by linker peptides to form cylindrical structures, or rods, that assemble to form PBS complex superstructures that can associate with PSII or PSI (**Fig. 1C**) (Arteni et al., 2009; Liu et al., 2013). Four different classes of PBS complexes have been identified, which are defined based on their shape: (1) hemi-discoidal (the most common shape) (Glazer, 1983), (2) hemi-ellipsoidal (Gantt and Lipschultz, 1972), (3) bundle-shaped (Guglielmi et al., 1981) and (4) rod-shaped (Marquardt et al., 1997; Hirose et al., 2019). All PBS complexes that are associated with PSII are comprised of two substructures: a core that is always made up of APC and a suite of rods arising out the core, which may contain PC, PC and PEC, and/or PE depending on species and growth environment (Ho et al., 2017; 2019).

For PSII-associated PBS complexes, four main groups of linker peptides have been identified: (1) rod linker proteins (27-35 kDa) that connect $(\alpha\beta)_6$ hexamers to form a rod, (2) a rod capping linker (8-11 kDa) that terminates rod elongation at the rod-end distal to the core, (3) a rod-core linker (25-29 kDa) that connects the rod to the core, and (4) a core-membrane linker (70-120 kDa) that connects the core to a thylakoid-embedded PSII (Liu et al., 2005; Gao et al., 2011; Watanabe and Ikeuchi, 2013; Zhang et al., 2017; Elanskaya et al., 2018; Rast et al., 2019). Most linker proteins do not contain chromophores and are colourless. However, in species that produce PE, a unique chromophorylated rod linker protein (called the γ-subunit) sits within the PE hexamer and facilitates rod formation through interaction with rod linker proteins in neighbouring $(\alpha\beta)_6$ hexamers (Zhang et al., 2017; Vásquez-Suárez et al., 2018). Distinct rod-shaped PBS complexes that do not contain APC have also been described in association with PSI. In this case, a unique CpcL linker protein connects the rod directly to PSI (**Fig. 1C**) (Watanabe et al., 2014; Hirose et al., 2019; Niedzwiedzki et al., 2019).

Mesophilic PBS complexes in red algae and cyanobacteria have been shown to be mobile, and can dissociate from and re-associate with different photosystems to balance the energy

distribution between PSI and PSII (i.e. state 1-state 2 transitions) (Mullineaux et al., 1997; Kaňa et al., 2014). However, the mechanisms and regulation involved in this process remains unclear (Calzadilla et al., 2019; Liu and Blankenship, 2019). More recently, cryo-electron tomography work has revealed that PBS complexes in the model cyanobacterium *Synechocystis* sp. PCC 6803 (PCC 6803) cluster on the thylakoid membrane as linear arrays of up to 20 PBSs that are linked by the peripheral PC rods and APC core, suggesting the possibility of additional linkage sites between PBS complexes (Rast et al., 2019). For further details on PBS structure, assembly and function, we recommend several recent reviews (Saer and Blankenship, 2017; Bryant and Caniffe, 2018; Harris et al., 2018; Adir et al., 2019; Li et al., 2019a).

Phycobiliproteins in thermophiles

Temperature has a major impact on the functionality and efficiency of the components of the light reactions of photosynthesis. Nevertheless, hyperthermophilic cyanobacteria found in alkaline hot springs are the dominant primary producers and flourish near the upper temperature limits for phototrophic life (*ca*. 73 °C) (Castenholz, 1969; Miller and Castenholz et al., 2000; Madigan et al., 2018). Four hyperthermophilic strains of the unicellular cyanobacterium *Synechococcus* spp., OH28, OH29 and OH30 (isolated from Hunter's Hot Springs, Oregon) and *Synechococcus lividus* sp. SyI (isolated from the lower geyser basin at the Yellowstone National Park, Wyoming) have optimal growth temperatures above 60 °C and currently hold the record for maintaining long-term autotrophic growth (i.e. active PBS-associated photosystems) at 70 °C (**Table 1**) (Edwards et al., 1996; Miller and Castenholz et al., 2000; Pedersen and Miller, 2017). Furthermore, several other unicellular thermophilic cyanobacteria have been shown to grow optimally at 45-60 °C, including *Synechococcus lividus* PCC 6715, *Thermosynechococcus vulcanus* NIES 2134, *Thermosynechococcus elongatus* NIES 2133 (also known as BP-1), *T. elongatus* TA-1 and more recently *T. elongatus* PKUAC-SCTE542 (Onai et al., 2004; Leu et al., 2013; Liang et al., 2018; 2019). There are also several examples of multicellular cyanobacterial thermophiles, such as the true branching, nitrogen-fixer *Fischerella thermalis* (also known as *Mastigocladus laminosus*), which is found in microbial mats of hot springs at temperatures of up to 69 °C (Alcorta et al., 2018; 2019).

The thermostability of PBPs from thermophilic species has been examined both *in vitro* and *in vivo*, with PC being the most well characterised PBP. In thermophiles, the coupling of PBS

to photosystems is stronger than in mesophiles, such that thermophiles rely more on non-photochemical quenching than state transitions to regulate light capture efficiency (Kaňa et al., 2014). However, prolonged exposure to extreme temperatures can still result in the reversible dissociation of PBSs from photosystems or, under severe stress, irreversible denaturation of PBP components (Pedersen and Miller, 2017; Alcorta et al., 2019). The structural state of the PBS can be inferred from the amplitudes of its PBP absorbance or fluorescence peaks, which are dependent on the rigid conformation of the attached bilin chromophore(s) in the folded biliprotein (Ma et al., 2007). When a PBP denatures the chromophore typically remains attached to protein, but its absorbance and fluorescence peaks are either significantly reduced or disappear owing to losses in chromophore rigidity (Kupka and Scheer, 2008).

The concentration of PC extracted from the mesophilic species *A. platensis* has been shown to decline with increasing temperatures (i.e. in terms of absorbance, indicative of protein denaturation), with 22% and 48% losses following incubation at approximately 50 °C and 60 °C, respectively, for 30 minutes at pH 7 (Patel et al., 2004; Chaiklahan et al., 2012; Wu et al., 2016). In contrast, PC extracted from *S. lividus* PCC 6715 showed only a 15% loss at 60 °C for 5 hours at pH 7, and no losses at 50 °C for 4 hours within a pH range of 4 to 8 (Liang et al., 2018). Measurements based on fluorescence of PC extracted from *T. elongatus* TA-1 also showed minimal losses of PC (i.e. ~10%) following incubation at 50 °C for 4 hours within a wider pH range of 4 to 9 (Leu et al., 2013), indicating that PC from *T. elongatus* TA-1 may have more robust pH stability compared to that from *S. lividus* PCC 6715. Fluorescence is a more sensitive method of measuring PC stability compared to absorbance (Kupka and Scheer, 2008; Stoitchkova et al., 2007), and stability measurements between *in vitro* absorbance- and fluorescence-based studies may not be directly comparable, but the observed trends clearly show that PC from thermophilic species is stable for longer at higher temperatures and often in a wider pH range. To date, the most thermostable PC examined *in vitro* was isolated from *S. lividus* sp. SyI (Edwards et al., 1997). Although limited information is available regarding the testing conditions, PC extracted from *S. lividus* sp. SyI reportedly remained stable at *ca*. 70 °C.

Reconstruction of the assembly pathway for PBPs in *E. coli* has allowed for further *in vitro* characterisation studies (Tooley et al., 2001), for example, of APC subunits from thermophilic species (Chen et al., 2013). Fluorescence of heterologously produced APC β-

subunit from *T. elongatus* BP-1 showed long-term stability (i.e. no change following storage at 4 °C for 30 days) and was reduced by 30% following a 4-hour incubation at 60 °C. In contrast, the fluorescence of the APC β-subunit from the mesophilic model species PCC 6803 was reduced by over 90% following either long-term storage or short-term incubation at 60 °C. The APC □-subunit in *T. elongatus* BP-1 and PCC 6803 was relatively more stable for both species, as fluorescence decreased by 5% and 60%, respectively, following a 1-hour incubation at 65 °C (Chen et al., 2016). Notably, maximum fluorescence of the APC □-subunit from *T. elongatus* BP-1 was observed at a slightly higher pH range (pH 7 to 9) compared to PCC 6803 (pH 5 to 7). *T. elongatus* species are typically found in alkaline hot springs and grow better at pH 9, which suggests that APC □-subunits can be adapted to different pH environments (Leu et al., 2013).

To better understand the stability adaptations of photosystems and PBS to different thermal environments, several authors have investigated the interactions between PSII and PBS using *in vivo* fluorescence approaches (Pedersen and Miller, 2017). Under standard growth conditions, PBSs are tightly coupled to PSII such that excitation energy from light is directed to the photosynthetic reaction centre, and the only minimal levels of fluorescence are observed for individual PBP components (e.g. PC or APC). However, environmental changes such as increases in temperatures can lead to PSII inactivation, disassociation of PBSs, and eventually PBP denaturation, with consequent changes in the associated PBP fluorescence peaks. Notably, the temperatures required for PSII and PBS inactivation typically exceed the thermal limits for sustained growth for cyanobacterial strains, which indicates an adaptive capacity of the light reactions to short-term high temperature stress (Miller and Castenholz, 2000; Allewalt et al., 2006). In PCC 6803, PSII was fully inactivated after 5 minutes at 52 °C as evidenced by a decrease in fluorescence of PSII (i.e. at 690 nm measured at 77K) (Stoitchkova et al., 2007). Subsequent dissociation of the PBS resulted in an increase in the fluorescence peaks of individual PBP components (i.e. PC at 650 nm and APC at 660 and 685 nm). PBPs in PCC 6803 appeared to remain stable and highly fluorescent until 64 °C *in vivo*, after which fluorescence declined, indicative of protein denaturation. The latter was observed in a similar temperature range where a decline in absorbance was observed for PC from *A. platensis in vitro* (Chaiklahan et al., 2012). In contrast, *in vivo* fluorescence of PC and APC in *T. vulcanus* did not change following incubation at 70 °C for 5 minutes, and increased fluorescence (indicating PBS disassociation from PSII) was only observed at 80 °C

(Inoue et al. 2000). Incubation at 90 °C for 5 minutes eventually led to a significant reduction in PC fluorescence while APC fluorescence was no longer detectable. The latter result could indicate that PC is more thermostable than APC. Inactivation of PSII started at 55 °C but was only completely inactivated at 68 °C. Notably, *T. vulcanus* cells showed partial recovery of PSII activity from short exposure to high temperatures (i.e. up to 74 °C for 5 minutes) when cooled to 50 °C. However, in comparison to PC and APC, these results suggest that PSII in *T. vulcanus* is significantly more heat sensitive and thus, like PCC 6803, PSII is the more limiting factor restricting photosynthetic efficiencies at high temperatures.

Whole cell *in vivo* fluorescence measurements of *Synechococcus* OH28 have shown the most remarkable adaptation to high temperatures stress with PBS and PSII inactivation occurring at 75 °C and at 80 °C, respectively (Pedersen and Miller, 2017). To date, *Synechococcus* OH28 is the only cyanobacterial strain identified where PSII appeared more thermostable than the PBS. The latter may be a phenotypic trait that evolved under the acutely high temperatures (*ca*. 70 °C) in their native habitat (Miller and Castenholz et al., 2000). However, *Synechococcus* OH28 also demonstrated a relative reduction in photochemical efficiencies (i.e. an increase in fluorescence) at temperatures below 60 °C, which may be due to partial PBS disassociation at lower temperatures (Pedersen and Miller, 2017). A similar phenomenon has been observed in the thermophilic red alga *Cyanidium caldarium*, where the PBS was coupled to PSII at 38 °C but dissociated at lower temperatures (i.e. 14 °C) resulting in a subsequent increase in PBP fluorescence (Kana et al., 2014). These data suggest a structural evolutionary trade-off between the capacity for PSII and PBS coupling and adaptation to high temperature environments (Pedersen and Miller, 2017).

Structural characteristics of thermostable phycocyanin

The structure and composition of PC has been extensively studied, and several studies have examined how specific residues contribute to increased structural rigidity and thermostability in thermophilic species (Adir et at al., 2001; Pittera et al., 2017; Liang et al., 2018). Notably, the degree of homology between PC α- and β-subunits from different species is high, while crystal structures from a variety of species have shown a great deal of similarity (Adir et at al., 2001). Recent sequence analysis of the differences between PC subunits from 21 cold- (i.e. 10-25 °C) and warm-adapted (i.e. 18-35 °C) marine *Synechococcus* strains revealed two common substitutions (Pittera et al., 2014; Pittera et al., 2017). Firstly, a glycine to alanine substitution (i.e. a more hydrophobic amino acid) was identified at residue 43 (G43A) on α-

helix B of the □-subunit in warm-adapted strains (**Fig. 2**). Subsequent analysis of the substitution region (i.e. residues 35-45) predicted a decrease in flexibility of the peptide backbone in warm-adapted strains (Gasteiger et al., 2005), which was in agreement with the more rigid conformations observed for thermophilic strains (Akanuma et al., 2019). Notably, hyperthermophilic species also contain a hydrophobic residue (valine) at this position. In addition, residue 43 faces the β-subunit and might influence the stability of the (□β) monomer. Secondly, a serine to asparagine substitution was identified at residue 42 (S43N) on the β-subunit in warm-adapted strains. Residue 42 is located on an exposed domain of □-helix C, which faces helix I of the □-subunit of a neighbouring (□β) monomer within the hexameric $(□β)_6$ complex. The thermostability of PC assemblies (i.e. $(□β)_3$ or $(□β)_6$ complexes) are significantly higher than the (□β) monomer (Edwards et al., 1997). Therefore, amino acid substitutions on the interface between □- and β- subunits, (□β) monomers and $(□β)_3$ trimers are likely to impact on the stability of the entire PBS assembly, particularly as each substitution will be repeated six times within each $(□β)_6$ PC hexamer.

Further structural comparisons of the $(□β)_6$ PC hexamers from cyanobacterial species from different habitats revealed three symmetrical "hot spots" that potentially contribute to thermostability (**Fig. 3A, 3B**) (Liang et al., 2018). The hot spots included five residue substitutions located on □-helix B of the □-subunit at positions 21, 28, 33, 37 and 42, and one at position 145 (**Fig. 2**; **Fig. 3C**, **3D**). In thermophilic species, these residues form additional hydrogen bonds and salt bridges either with other residues within the □-subunit, with the β-subunit of its (□β) monomer, or with the □-subunit of the opposite $(□β)_3$ trimer that is positioned in a face-to-face orientation within the $(□β)_6$ hexamer (**Fig. 3D**).

A further residue change in the hyperthermophilic species *Synechococcus* OH28 was identified on the □-subunit of PC, consisting of a glutamine (or leucine) to methionine substitution at residue 111 (Q/L111M) when compared to the slightly less thermophilic strain *Synechococcus* OH20 or several mesophilic species (**Table 1**; **Fig. 2**). The methionine substitution was shown to make contact with the PCB chromophore on cysteine residue 84 on the □-subunit (□84), and has been attributed to the blue shift in the absorption peak of PC (i.e. from 620 nm to 608 nm) observed in *Synechococcus* OH28 (a relatively unique phenotypic trait also observed in the hyperthermophile *S. lividus* sp. SyI) (Edwards et al., 1996; Pedersen and Miller, 2017). Although the specific impact of this residue change on PC

stability is not clear, this was the only modification identified as under positive selection using a maximum-likelihood model of codon evolution in a range thermophilic *Synechococcus* species.

Phycobiliproteins in thermoacidophiles

To date, no cyanobacterial species have been identified in environments of pH less than 4 (Hirooka et al., 2017). However, several eukaryotic photosynthetic species can be found in such niches. Here we have highlighted the two genera of red algae *Galdieria* and *Cyanidioschyzon* as examples of PBS-containing microorganisms that prosper in thermoacidophilic conditions (i.e. pH 0.05-5 at 42-56 °C) (De Clerck et al. 2012; Reisser, 2013; Miyagishima et al., 2017; Ciniglia et al., 2019). For example, *Galdieria sulphuraria* is a polyextremophile with an impressive ability to survive at low pH (pH 1-5), a high temperatures (up to 56 °C), high salt (up to 10% [w/v] NaCl, three-fold higher than sea water) and in the presence of toxic metals (e.g. cadmium, mercury, aluminum, and nickel) (Weber et al., 2004; Seckbach, 2005; Reisser, 2013; Minoda et al., 2015; Hirooka and Miyagishima, 2016; Rossoni and Weber, 2019). Furthermore, *G. sulphuraria* can grow heterotrophically on over 50 different carbon sources, including sugars and sugar alcohols (e.g. glycerol and dulcitol). *Cyanidioschyzon merolae* is of interest as a model organism because of its unique position at the root of the red algal lineage as an intermediate between cyanobacteria and higher plants. In addition to a PBS complex associated with PSII, *C. merolae* also possesses a light-harvesting complex (LHC) associated with PSI, synonymous with the LHC present in green algae and higher plants (Nikolova et al., 2017).

Thermoacidophilic red algae have also evolved PBPs with robust stability under high temperatures, comparable to that of thermophilic cyanobacteria. For example, the absorbance of PC extracted from *G. sulphuraria* was reduced by *ca.* 20% after incubation at 70 °C for 30 minutes at pH 4.5 (Moon et al. 2014), while the absorbance of PC extracted from *C. merolae* did not decrease following incubation at 70 °C for 30 minutes at pH 5, and was reduced only by 30% after incubation at 80 °C (Rahman et al. 2017). Interestingly, the PC □-subunit of *C. merolae* has two extra cysteine residues at positions 27 and 73, which are also present in hyperthermophiles (**Fig. 2**). These residues may form covalent disulphide bonds and thus increase the stability of the protein (Fass, 2012; Rahman et al., 2017).

Acidophiles maintain an intracellular pH close to neutral (comparable to mesophilic species) through several adaptations, including a plasma membrane with reduced permeability to protons, active ATP-dependent proton export, and/or coupled export, where a symporter or antiporter uses the driving force of a different ion to remove protons (Beardall and Entwisle, 1984; Messerli et al., 2005; Enami et al., 2010; Madigan et al. 2018). Thus, PBPs from acidophiles are generally not exposed to acidic environments, such that PBPs extracted from acidophilic species show similar stability characteristics to mesophilic species under low pH conditions (Patel et al., 2004; Antelo et al., 2008; Chaiklahan et al., 2012; Patel et al., 2018).

PBPs from mesophilic species are typically stable at room temperature within a pH range of 4 to 8, and are most stable at pH 5 when exposed to increased temperatures (Patel et al., 2004; Antelo et al., 2008; Chaiklahan et al., 2012; Patel et al., 2018). However, incubation of PC from *A. platensis* at pH less than 4 led to conversion of the rigid, extended conformation of the bilin chromophores into cyclic forms and subsequent chromophore protonation, resulting in a shift in a peak absorption from 620 nm to 650-700 nm and a change in pigment colour from blue to green (Falkeborg et al., 2018). Incubation at low pH (i.e. pH 3) at room temperature also led to rapid protein denaturation, as evidenced by a 70% reduction in PC absorbance (Wu et al., 2016). Similarly, PC extracted from *C. merolae* (grown in pH 2 media) was generally stable under room temperature condition at pH 4, but the absorbance of PC rapidly dropped to 50% at pH 3 (Rahman et al., 2017). Analogous results were observed for PC from two acidophilic strains of *Galdieria spp*. (Carfagna et al., 2018). Thus, PBPs appear able to evolve in response to a wide range of temperature environments, but show a limited capacity to adapt to different pH conditions, particularly low pH. The latter may be due to limits in the evolutionary capacity of the PBS, or possibly because PBPs from acidophiles have not been subjected to suitable selection pressure.

Applications of phycobiliproteins with increased stability

PBPs may be useful in a wide variety of industrial applications. At present, only mesophilic species are used for commercial production of PBPs: two strains of red algae for the production of PE (i.e. *Porphyridium* sp. and *Rhodella* sp.), while PC is produced exclusively from the cyanobacteria *Arthrospira* spp. (Spolaore et al., 2006). However, many industrial processes operate under conditions that exceed the stability range of PBPs sourced from mesophiles. Here, we briefly review applications that could take advantage of the superior properties of PBPs from extremophilic species with an emphasis on the food and textile

industries. Finally, we consider some of the challenges in large scale production and purification of thermophilic PBPs.

Food colourants

Synthetic food colourants, such as Ponceau 4R and Allura Red AC, have been increasingly criticised for their potential negative impact on human health, and particularly for their association with the attention deficit hyperactivity disorder (ADHD) in susceptible children (McCann et al., 2007; Coultate and Blackburn, 2018). Subsequent marketing pressures have spurred the food industry to replace the use of synthetic colourants with biologically-derived 'natural 'pigments, such as anthocyanins and carotenoids, with an accompanying promotion of their apparent health benefits (Li et al., 2017; Eggersdorfer and Wyss, 2018). The global demand for natural food colourants is currently increasing at a significant rate, with the total market revenue expected to grow by 6% annually over the period 2015-2025 from USD 1.94 billion in 2018 (Research and Markets, 2019).

The two PBPs PC and PE have been extensively used as blue and red colourants, respectively. PC from *A. platensis* is particularly important for the food industry as it is currently the only known natural, soluble blue colourant (Coultate and Blackburn, 2018). PC has been used for colouration of many types of foods, but primarily for confectionaries and dairy products, such as ice-cream and yoghurt (Eriksen et al., 2008). *A. platensis* is currently the only cyanobacterium that has GRAS (generally recognised as safe) status, and the use of PBS components from *A. platensis* as colour additives are currently exempt from the certification by the U.S. Food and Drug Administration (FDA) in some but not all food goods (Code of Federal Regulations Title 21, 2019). A critical barrier to the commercial usage of PC or PE from thermophiles is the need for the source organism to obtain administrative approval (e.g. GRAS status from the FDA), which requires a significant capital investment to perform extensive toxicological testing. Nevertheless, the applications of *A. platensis* PC in the food industry remain limited due to its relatively low thermostability. For instance, low temperature or batch pasteurisation conditions typical for dairy products (e.g. 62 °C for 30 minutes) would result in significant losses of *A. platensis* PC (Antelo *et al.*, 2008; Chaiklahan *et al.*, 2012). In contrast, PC from thermoacidophilic red alga *C. merolae* would be 100% stable under those conditions (Rahman et al., 2017).

Usage of PBPs in the food industry is also limited by pH. For example, the majority of beverages in the drinks and beverage industry have a pH below 4, which is currently beyond the long-term stability range of PC from both mesophilic and extremophilic species (Reddy et al., 2017). Nevertheless, the demand for beverages with natural blue colourants remains high (Galaup et al., 2019). Thus, the identification of native PCs or engineering of synthetic variants (e.g. using directed evolution approaches in *E. coli*) with improved pH stability could have significant commercial applications.

Many attempts have been made to improve the stability of mesophilic PBPs using a range of additives, such as acids, sugars, salts and cross-linking agents (**Table 2**). The majority of the studies have utilised additives that are already widely used in the food industry and comply with FDA safety regulations. For example, the thermostability of *A. platensis* PC can be increased by the addition of sugars, such as fructose or glucose, which facilitate protein polymerisation via the formation of N-linked glycosidic bonds (Martelli et al., 2014; Hadiyanto et al., 2018). Common food preservatives, such as citric and benzoic acids, have also been shown to improve the thermostability of PC, which may be linked to a reduction in pH of the solution to levels that favour stability (e.g. pH 5.5) (Mishra et al., 2008; Mogany et al., 2019).

Toxic additives, such as cross-linking agents (e.g. glutaraldehyde, formaldehyde and dithiobis (succinimidyl propionate)) can also significantly improve the stability of PBPs for application uses outside of the food industry, such as fluorescent labels used in biomedical research (Cubicciotti, 1997; Fukui et al., 2004; Sun et al., 2006). Fusion proteins of PC □-subunit were used to prevent dissociation of PC $(□β)_3$ trimers into (□β) monomers at low protein concentration (Cai et al., 2001). PBPs can also be stabilised by protein fusion tags, microencapsulation techniques (e.g. using alginate and chitosan) or by the formation of nanofibers using synthetic polymers (e.g. polyethylene oxide) (Cai et al., 2001; Yan et al., 2014; Braga et al., 2016; Pradeep and Nayak, 2019). Recently, improved stability of PC at pH 2 was demonstrated using sodium dodecyl sulphate (SDS) micelles, which prevented protonation of the chromophore(s) and thus preserved the blue colour (Falkeborg et al., 2018). Notably, there are no studies to our knowledge that have attempted to further improve the stability of PBPs from thermophilic species. Augmenting the superior properties of PBPs from thermophilic species with stabilising additives could significantly expand the applications of PBPs in the food industry and beyond.

Textiles dyes

The textile industry primarily relies on synthetic dyes produced from chemicals, petroleum by-products, and minerals. The negative environmental impact of synthetic dyes is well recognised, particularly in terms of water pollution (Kant, 2012). Natural dyes offer several advantages in terms of sustainability, including a reduced carbon footprint for the textile industry (Moldovan et al., 2017a). However, the uptake of natural dyes, such as PBPs, is still limited due to challenges in colour and shade reproduction, poor fastness (i.e. resistance to fading or running) to washing detergents and light exposure (Khatri and White, 2015). Recent studies have demonstrated that cotton fabrics coloured with PE-based dyes from the mesophilic red algae *Gracilaria cornea* and *Gracilaria gracilis* do comply with the European accepted standards (UNE-EN ISO) for textiles in terms of colour and fastness to laundering and rubbing tests (e.g. the measurement of the durability of a fabric) (Moldovan et al., 2017a, b). Furthermore, PC from *A. platensis* and PE from the mesophilic red macroalga *Gracilaria vermiculophylla* has also been used successfully for dyeing cotton and wool fabrics (Ferrandiz et al., 2016; Gorman et al., 2017).

In the course of the dyeing process, textiles are often subjected to high temperatures in the dye solution (e.g. 90 minutes at 50 °C) (Ferrandiz et al., 2016). During cotton printing, the attachment of the dye to the fabric requires drying at 80 °C for 10 minutes, followed by curing at 110 °C for 2 minutes (Moldovan et al., 2017a, b). The latter process leads to a reduction in colour intensity for PE from *Gracilaria* sp. , indicative of PBP degradation. As an alternative, PC from thermophilic *S. lividus* PCC 6715 has shown robust stability under prolonged temperature stress and may remain stable upon short-term exposure to curing temperatures (Liang et al., 2018). The usage of natural dyes, such as PBPs, in the textile industry is still developing, but we hypothesise that improvements in PBP performance and access to sufficient quantities of substrate could provide an eco-friendly, biodegradable, non-carcinogenic and sustainable alternative to synthetic dyes.

Other potential applications

PBPs could be of significant use as natural alternatives to chemical sensitising dyes in low cost photovoltaics devices, such as dye-sensitised solar cells (Bora et al., 2012; Schrantz et al., 2017; Sharma et al., 2018; Li et al., 2019a). However, long-term stability would be required under direct sunlight and at temperatures up to 80 °C. PBPs have also shown

promise in pharmaceutical research as a potent anti-oxidant (Dejsungkranont et al., 2017; Li et al., 2019b). But their applications are limited due to the loss of the anti-oxidant functionality during long-term storage (Mishra et al., 2008; Chen et al., 2016; Yang et al., 2017). PC in particular, has been considered as a promising anti-cancer agent against multiple types of cancer cells (for a detailed review see Jiang et al., 2017). Lastly, PBPs have several important advantages relative to other fluorescent labels used in research and diagnostics, including a smaller size (i.e. 27 kDa for GFP compared to *ca*. 18 kDa for a PC □-subunit) and a higher quantum yield (e.g. PC □-subunit carrying PEB chromophore (0.98) compared to mCherry (0.22) or eGFP (0.60)) (Alvey et al., 2011; Wall et al., 2015; Chen and Jiang, 2018). PBPs from thermophilic species show significant promise for specific fluorescent labelling applications, such as *in situ* protein localisation studies where elevated temperatures are required (e.g. to study autotrophic and heterotrophic thermophiles) (Frenzel et al., 2018).

Production and extraction of phycobiliproteins

The levels of PC productivity from *A. platensis* typically vary between 14 and 125 mg L^{-1} d^{-1} depending on the growth conditions (e.g. light, temperature and nitrogen availability) (Chen et al. 2013; Ho et al., 2018; Lima et al., 2018; Pagels et al., 2019). In comparison, the highest reported productivity for a thermostable PC from cyanobacteria is much lower (*ca*. 0.25 mg L^{-1} d^{-1}, from *S. lividus* PCC 6715) (Liang et al., 2018). Thus, significant improvements are required to match the production capacity for commercial strains. To date, the highest yield of PBP achieved in *E. coli* is 56.4 mg L^{-1} d^{-1} (*ca.* 37% of the total cell protein) for the APC □-subunit from *T. elongatus* BP-1, in which 96.7% of the PBPs carried a covalently attached chromophore (Chen and Jiang, 2019). As APC concentrations are up to eight-fold lower than PC in native PBSs (e.g. from *A. platensis*), *E. coli* appears a promising chassis for heterologous production of thermostable PBP subunits. Assembly of APC $(□\beta)_3$ trimers has also been demonstrated in *E. coli*, but potential yields have not yet been reported (Liu et al., 2010).

In red alga *C. merolae* the reported PC productivity was low (0.016 mg L^{-1} d^{-1}) owing to a low PC content of 0.31 mg g^{-1} of cell dry weight (Rahman et al., 2017). In contrast, a remarkably high PC productivity of 2.2 g L^{-1} d^{-1} has been reported in *G. sulphuraria* 074G using a combination of heterotrophic and phototrophic conditions to achieve a high cell density and induce PC production, respectively (Wan et al. 2016). However, the growth

medium (pH 2.0) and high temperatures (up to 56 °C) required to cultivate *G. sulphuraria* can lead to rapid corrosion of commonly used stainless steel bioreactors and increased energy consumption, making large-scale production more challenging (Eriksen, 2018).

Improving the productivity of PBPs from thermophilic species could be achieved by optimising growth conditions and media composition (del Rio-Chanona et al., 2015; Lima et al., 2018; Mogany et al., 2018). However, an alternative strategy could lie in engineering PBPs from extremophilic species into faster growing, genetically amenable species (e.g. PCC 6803, *Synechococcus elongatus* UTEX 2973 or *Synechococcus* sp. PCC 11901) (Yu et al., 2015; Włodarczyk et al., 2019), or by designing synthetic biliproteins with the necessary properties *de novo* (Mancini et al., 2017; Sheehan et al., 2018; Dawson et al., 2019). An increasing availability of synthetic biology tools in cyanobacteria could help to further increase PBP production as well as understand PBS stability properties (Gale et al., 2019; Vasudevan et al., 2019). Genetic engineering of novel PBP variants into *A. platensis* would be an ideal scenario considering its GRAS status, high achievable yields of PBPs, favourable conditions for preventing growth of contaminants (i.e. culturing at pH 8-11.5) in open raceways and the vast amount of studies regarding downstream processing and protein extraction. However, transformation of *A. platensis* has proved challenging due to the presence of robust native endonuclease activities, which greatly restrict transformation efficiencies and prevent the uptake of heterologous DNA (Tragut et al., 1995; Shiraishi and Tabuse, 2013; Jeamton et al., 2017). There are also several maintenance challenges associated with *A. platensis* cultivation. For example, *A. platensis* requires a high concentration of inorganic salts for optimal growth, which can decrease the solubility of CO_2 in the media (da Rosa et al., 2015). Furthermore, growth in an alkaline pH reduces the solubility of metal ions (e.g. Fe and Mg) that play a key role in cyanobacterial growth (Nogami et al., 2016). Therefore, production of PBPs in alternative species should be considered.

Finally, strategies to improve the scale and efficiency of downstream processing for *A. platensis* biomass and PC extraction have been studied extensively over the past several decades (de Jesus et al., 2016). Traditional inexpensive and rapid biomass processing methods, such as spray drying (i.e. short term exposure to 150 °C) or oven drying (i.e. 7 hours at 60 °C), resulted in *ca*. 50% losses of *A. platensis* PC (Sarada et al., 1999). Although comparable studies from thermophilic species are still lacking, biomass from the latter will

likely perform significantly better in extraction methods that require high-temperature conditions.

Closing remarks

PBSs are remarkable pigment protein complexes that have successfully evolved to maintain functionality in extreme temperature conditions. The potential roles of specific residues in the thermostability of PBPs have provided target sights for the screening of novel thermotolerant isoforms. With the vast accumulation of structural data for PBSs and PBPs, the rapid emergence of new molecular tools available for cyanobacterial research should help researchers to test the contributions of particular residues and even design new synthetic PBP variants. In this context, extremophilic species play a vital role as a source of genetic variation to develop hypotheses to test the capacity of PBS components to adapt to different environments. Moreover, several industries could benefit from taking advantage of the thermostability of PBPs from extremophiles, particularly when used in combination with other approaches that could further improve performance.

Acknowledgements

AJM acknowledges funded from the UKRI Biotechnology and Biological Sciences Research Council (BBSRC) (grant number BB/S020128/1), the Industrial Biotechnology Innovation Centre (IBioIC) and industrial collaborator ScotBio. AP was funded by the BBSRC National Productivity Investment Fund (NPIF) - IBioIC Collaborative Training Partnership (CTP) programme (grant number BB/R505511/1) with ScotBio.

References

Adir N. 2005. Elucidation of the molecular structures of components of the phycobilisome: reconstructing a giant. Photosynthesis Research **85**, 15-32.

Adir N, Bar-Zvi S and Harris D. 2019. The amazing phycobilisome. Biochimica et Biophysica Acta (BBA)-Bioenergetics, 148047.

Adir N, Dobrovetsky Y and Lerner N. 2001. Structure of C-phycocyanin from the thermophilic cyanobacterium *Synechococcus vulcanus* at 2.5 Å: structural implications for thermal stability in phycobilisome assembly. Journal of Molecular Biology **313**, 71-81.

Akanuma S, Bessho M, Kimura H, Furukawa R, Yokobori SI and Yamagishi A. 2019. Establishment of mesophilic-like catalytic properties in a thermophilic enzyme without affecting its thermal stability. Scientific Reports **9**, 9346.

Alcorta J, Espinoza S, Viver T, Alcamán-Arias ME, Trefault N, Rosselló-Móra R and Díez B. 2018. Temperature modulates *Fischerella thermalis* ecotypes in Porcelana Hot Spring. Systematic and Applied Microbiology **41**, 531-543.

Alcorta J, Vergara-Barros P, Antonaru LA, Alcamán-Arias ME, Nürnberg DJ and Díez B. 2019. *Fischerella thermalis*: a model organism to study thermophilic diazotrophy, photosynthesis and multicellularity in cyanobacteria. Extremophiles **23**, 1-13.

Allewalt JP, Bateson MM, Revsbech NP, Slack K and Ward DM. 2006. Effect of temperature and light on growth of and photosynthesis by *Synechococcus* isolates typical of those predominating in the octopus spring microbial mat community of Yellowstone National Park. Applied and Environmental Microbiology **72**, 544-550.

Alvey RM, Biswas A, Schluchter WM and Bryant DA. 2011. Attachment of noncognate chromophores to CpcA of *Synechocystis* sp. PCC 6803 and *Synechococcus* sp. PCC 7002 by heterologous expression in *Escherichia coli*. Biochemistry **50**, 4890-4902.

Antelo FS, Costa JAV and Kalil SJ. 2008. Thermal degradation kinetics of the phycocyanin from *Spirulina platensis*. Biochemical Engineering Journal **41**, 43-47.

Arteni AA, Ajlani G and Boekema EJ. 2009. Structural organisation of phycobilisomes from *Synechocystis* sp. strain PCC 6803 and their interaction with the membrane. Biochimica et Biophysica Acta (BBA) - Bioenergetics **1787**, 272-279.

Beale SI. 1994. Biosynthesis of Cyanobacterial Tetrapyrrole Pigments: Hemes, Chlorophylls, and Phycobilins. In: Bryant DA, eds. The Molecular Biology of Cyanobacteria. Advances in Photosynthesis. Dordrecht: Springer, 519-558.

Beardall J and Entwisle L. 1984. Internal pH of the obligate acidophile *Cyanidium caldarium* Geitler **23**, 397-399.

Bekasova OD, Borzova VA, Shubin VV, Kovalyov LI, Stein-Margolina VA and Kurganov BI. 2016. An increase in the resistance of R-phycoerythrin to thermal aggregation by silver nanoparticles synthesized in nanochannels of the pigment. Applied Biochemistry and Microbiology **52**, 98-104.

Bekasova OD, Shubin VV, Safenkova IV, Kovalyov LI and Kurganov BI. 2013. Structural changes in R-phycoerythrin upon CdS quantum dot synthesis in tunnel cavities of protein molecules. International Journal of Biological Macromolecules **62**, 623-628.

Blot N, Wu XJ, Thomas JC, Zhang J, Garczarek L, Böhm S, Tu JM, Zhou M, Plöscher M, Eichacker L and Partensky F. 2009. Phycourobilin in trichromatic phycocyanin from oceanic cyanobacteria is formed post-translationally by a phycoerythrobilin lyase-isomerase. Journal of Biological Chemistry **284**, 9290-9298.

Böcker L, Ortmann S, Surber J, Leeb E, Reineke K and Mathys A. 2019. Biphasic short time heat degradation of the blue microalgae protein phycocyanin from *Arthrospira platensis*. Innovative Food Science and Emerging Technologies **52**, 116-121.

Bora DK, Rozhkova EA, Scrantz K, Wyss PP, Braun A, Graule T and Constable EC. 2012. Functionalization of nanostructured hematite thin□film electrodes with the light harvesting membrane protein c-phycocyanin yields an enhanced photocurrent. Advanced Functional Materials **22**, 490-502.

Braga ARC, Figueira FDS, Silveira JTD, Morais MGD, Costa JAV and Kalil SJ. 2016. Improvement of thermal stability of C-phycocyanin by nanofiber and preservative agents. Journal of Food Processing and Preservation **40**, 1264-1269.

Bryant DA and Canniffe DP. 2018. How nature designs light-harvesting antenna systems: design principles and functional realization in chlorophototrophic prokaryotes. Journal of Physics B: Atomic, Molecular and Optical Physics **51**, 033001.

Cai YA, Murphy JT, Weemayer GJ and Glazer AN. 2001. Recombinant phycobiliproteins: recombinant C-phycocyanins equipped with affinity tags, oligomerization and biospecific recognition domains. Analytical Biochemistry **290**, 186-204.

Calzadilla PI, Zhan J, Sétif P, Lemaire C, Solymosi D, Battchikova N, Wang Q, Kirilovsky D. 2019. The cytochrome b6f complex is not involved in cyanobacterial state transitions. The Plant Cell **31**, 911-931.

Carfagna S, Landi V, Coraggio F, Salbitani G, Vona V, Pinto G, Pollio A and Ciniglia C. 2018. Different characteristics of C-phycocyanin (C-PC) in two strains of the extremophilic *Galdieria phlegrea*. Algal Research **31**, 406-412.

Carrieri D, Lombardi T, Paddock T, Cano M, Goodney GA, Nag A, Old W, Maness PC, Seibert M, Ghirardi M and Yu J. 2017. Transcriptome and proteome analysis of nitrogen starvation responses in *Synechocystis* 6803 Δ*glgC*, a mutant incapable of glycogen storage. Algal Research **21**, 64-75.

Castenholz RW. 1969. Thermophilic blue-green algae and the thermal environment. Bacteriological Reviews **33**, 476-504.

Chaiklahan R, Chirasuwan N and Bunnag B. 2012. Stability of phycocyanin extracted from *Spirulina* sp.: influence of temperature, pH and preservatives. Process Biochemistry **47**, 659-664.

Chen CY, Kao PC, Tsai CJ, Lee DJ and Chang JS. 2013. Engineering strategies for simultaneous enhancement of C-phycocyanin production and CO2 fixation with *Spirulina platensis*. Bioresource technology **145**, 307-312.

Chen H and Jiang P. 2018. Combinational biosynthesis and characterization of fusion proteins with tandem repeats of allophycocyanin holo-α subunits and their application as bright fluorescent labels for immunofluorescence assay. Journal of Bioscience and Bioengineering **126**, 778-782.

Chen H and Jiang P. 2019. Metabolic engineering of *Escherichia coli* for efficient biosynthesis of fluorescent phycobiliprotein. Microbial Cell Factories **18**, 58.

Chen H, Lin H, Li F, Jiang P and Qin S. 2013. Biosynthesis of a stable allophycocyanin beta subunit in metabolically engineered *Escherichia coli*. Journal of Bioscience and Bioengineering **115**, 485-489.

Chen H, Liu Q, Zhao J and Jiang P. 2016. Biosynthesis, spectral properties and thermostability of cyanobacterial allophycocyanin holo-α subunits. International Journal of Biological Macromolecules **88**, 88-92.

Chronakis IS. 2001. Gelation of edible blue-green algae protein isolate (*Spirulina platensis* strain Pacifica): thermal transitions, rheological properties and molecular forces involved. Journal of Agricultural and Food Chemistry **49**, 888-898.

Ciniglia C, Cennamo P, De Natale A, De Stefano M, Sirakov M, Iovinella M, Yoon HS and Pollio A. 2019. *Cyanidium chilense* (Cyanidiophyceae, Rhodophyta) from tuff rocks of the archeological site of Cuma, Italy. Phycological Research **67**, 311-319.

Cornejo J and Beale SI. 1988. Algal heme oxygenase from *Cyanidium caldarium*. Partial purification and fractionation into three required protein components. Journal of Biological Chemistry **263**, 11915-11921.

Cornejo J, Willows RD and Beale SI. 1998. Phytobilin biosynthesis: cloning and expression of a gene encoding soluble ferredoxin□dependent heme oxygenase from *Synechocystis* sp. PCC 6803. The Plant Journal **15**, 99-107.

Coultate T and Blackburn RS. 2018. Food colorants: their past, present and future. Coloration Technology **134**, 165-186.

Cubicciotti RS. 1997. Phycobilisomes, derivatives and uses therefor. U.S. Patent 5,695,990.

da Rosa GM, Moraes L, Cardias BB, Costa JA. 2015. Chemical absorption and CO2 biofixation via the cultivation of Spirulina in semicontinuous mode with nutrient recycle. Bioresource technology **192**, 321-327.

Dawson WM, Rhys GG and Woolfson DN. 2019. Towards functional *de novo* designed proteins. Current Opinion in Chemical Biology **52**, 102-111.

Dammeyer T and Frankenberg-Dinkel N. 2006. Insights into phycoerythrobilin biosynthesis point toward metabolic channelling. Journal of Biological Chemistry **281**, 27081-27089.

De Clerck O, Bogaert KA and Leliaert F. 2012. Diversity and evolution of algae: primary endosymbiosis. Advances in Botanical Research **64**, 55-86.

De Jesús VC, Guiérrez-Rebolledo GA, Hernández-Ortega M, Valadez-Carmona L, Mojica-Villegas A, Gutiérrez-Salmeán G and Chamorro-Cevallos G. 2016. Methods for extraction, isolation and purification of C-phycocyanin: 50 years of research in review. International Journal of Food and Nutritional Science **3**, 1-10.

De Marsac NT, 2003. Phycobiliproteins and phycobilisomes: the early observations. Photosynthesis Research **76**, 193-205.

Dejsungkranont M, Chen HH and Sirisansaneeyakul S. 2017. Enhancement of antioxidant activity of C-phycocyanin of Spirulina powder treated with supercritical fluid carbon dioxide. Agriculture and Natural Resources **51**, 347-354.

Del Rio-Chanona EA, Zhng D, Xie Y, Manirafasha E and Jing K. 2015. Dynamic simulation and optimization for *Arthrospira platensis* growth and C-phycocyanin production. Industrial and Engineering Chemistry Research **54**, 10606-10614.

Edwards MR, Hauer C, Stack RF, Eisele LE and MacColl R. 1997. Thermophilic C-phycocyanin: effect of temperature, monomer stability and structure. Biochimica et Biophysica Acta **1321**, 157-164.

Edwards MR, MacColl R and Eisele LE. 1996. Some physical properties of an unusual C-phycocyanin isolated from a photosynthetic thermophile. Biochimica et Biophysica Acta **1276**, 64-70.

Eggersdorfer M and Wyss,A. 2018. Carotenoids in human nutrition and health. Archives of Biochemistry and Biophysics **652**, 18-26.

Elanskaya IV, Zlenko DV, Lukashev EP, Suzina NE, Kononova IA and Stadnichuk IN. 2018. Phycobilisomes from the mutant cyanobacterium *Synechocystis* sp. PCC 6803 missing chromophore domain of ApcE. Biochimica et Biophysica Acta **1859**, 280-291.

Enami I, Adachi H and Shen JR. 2010. Mechanisms of acido-tolerance and characteristics of photosystems in an acidophilic and thermophilic red alga, *Cyanidium caldarium*. In Red Algae in the Genomic Age. Dodrecht: Springer, 373-389.

Eriksen NT. 2008. Production of phycocyanin—a pigment with applications in biology, biotechnology, foods and medicine. Applied Microbiology and Biotechnology **80**, 1-14.

Eriksen NT. 2018. Heterotrophic production of phycocyanin in *Galdieria sulphuraria*. In: Durvasula R, Subba Rao DV, eds. Extremophiles From Biology to Biotechnology. Heidelberg: CRC Press, 87-101.

Falkeborg MF, Roa-Serrat MC, Burnæs KL and Nielsen ALD. 2018. Stabilising phycocyanin by anionic micelles. Food Chemistry **239**, 771-780.

Fass D. 2012. Disulfide bonding in protein biophysics. Annual Review of Biophysics **41**, 63-79.

Ferrándiz M, Moldovan S, Mira E, Pinchetti JL G, Rodriguez T, Abreu H, Rego AM, Palomo B and Caro P. 2016. Phycobiliproteins – new natural dyes from algae as a sustainable method. Fibres and Textiles **3,** 56.

Frenzel E, Legebeke J, Van Stralen A, Van Kranenburg R and Kuipers OP. 2018. *In vivo* selection of sfGFP variants with improved and reliable functionality in industrially important thermophilic bacteria. Biotechnology for Biofuels **11**, 8.

Fukui K, Saito T, Noguchi Y, Kodera Y, Matsushima A, Nishimura H and Inada Y. 2004. Relationship between color development and protein conformation in the phycocyanin molecule. Dyes and Pigments **63**, 89-94.

Galaup C, Auriel L, Dubs J, Dehoux C, Gilard V, Poteau R, Retailleau E, Biasini G and Collin F. 2019. Blue wine, a color obtained with synthetic blue dye addition: two case studies. European Food Research and Technology **245**, 1777-1782.

Gale GA, Schiavon Osorio AA, Mills LA, Wang B, Lea-Smith DJ and McCormick AJ. 2019. Emerging species and genome editing tools: future prospects in cyanobacterial synthetic biology. Microorganisms **7**, 409.

Gantt E and Lipschultz C. 1972. Phycobilisomes of *Porphyridium cruentum*: I. Isolation. The Journal of Cell Biology **54**, 313-324.

Gao X, Zhang N, Wei TD, Su HN, Xie BB, Dong CC, Zhang XY, Chen XL, Zhou BC, Wang ZX and Wu JW. 2011. Crystal structure of the N-terminal domain of linker LR and the assembly of cyanobacterial phycobilisome rods. Molecular Microbiology **82**, 698-705.

Gasteiger E, Hoogland C, Gattiker A, Wilkins MR, Appel RD and Bairoch A. 2005. Protein identification and analysis tools on the ExPASy server. In: Walker JM, eds. The Proteomics Protocols Handbook. Humana Press, 571-607.

Glazer AN. 1984. Phycobilisome a macromolecular complex optimized for light energy transfer. Biochimica et Biophysica Acta **768**, 29-51.

Glazer AN. 1989. Lightguides. Directional energy transfer in a photosynthetic antenna. Journal of Biological Chemistry **264**, 1-4.

Glazer AN, Lundell DJ, Yaanaka G and Williams RC. 1983. July. The structure of a "simple phycobilisome". Annales de l'Institut Pasteur/Microbiologie **134**, 159-180.

Gonzalez-Ramirez E, Andujar-Sanchez M, Ortiz-Salmeron E, Bacarizo J, Cuadri C, Mazzuca-Sobczuk T, Ibáñez MJ, Camara-Artigas A and Martinez-Rodriguez S. 2014. Thermal and pH stability of the B-phycoerythrin from the red algae *Porphyridium cruentum.* Food Biophysics **9**, 184-192.

Gorman L, Kraemer GP, Yaish C, Boo SM and Kim JK. 2017. The effects of temperature on the growth rate and nitrogen content of invasive *Gracilaria vermiculophylla* and native *Gracilaria tikvahiae* from Long Island Sound, USA. Algae **32**, 57-66.

Guglielmi G, Cohen-Bazire,G. and Bryant DA. 1981. The structure of *Gloeobacter violaceus* and its phycobilisomes. Archives of Microbiology **129**, 181-189.

Hadiyanto, Christwardana M, Sutanto H, Suzery M, Amelia D and Aritonang RF. 2018. Kinetic study on the effects of sugar addition on the thermal degradation of phycocyanin from *Spirulina* sp. Food Bioscience **22**, 85-90.

Harris D, Bar-Zvi S, Lahav A, Goldshmid I and Adir N. 2018. The structural basis for the extraordinary energy-transfer capabilities of the phycobilisome. In: Harris J., Boekema E, eds. Membrane Protein Complexes: Structure and Function. Subcellular Biochemistry. Singapore: Springer, 57-82.

Hirooka S, Hirose Y, Kanesaki Y, Higuchi S, Fujiwara T, Onuma R, Era A, Ohbayashi R, Uzuka A, Nozaki H and Yoshikawa H. 2017. Acidophilic green algal genome provides insights into adaptation to an acidic environment. Proceedings of the National Academy of Sciences of The United States of America **114**, 8304-8313.

Hirooka S and Miyagishima SY. 2016. Cultivation of acidophilic algae *Galdieria sulphuraria* and *Pseudochlorella* sp. YKT1 in media derived from acidic hot springs. Frontiers in Microbiology **7**, 2022.

Hirose Y, Chihong S, Watanabe M, Yonekawa C, Murata K, Ikeuchi M and Eki T. 2019. Diverse chromatic acclimation processes regulating phycoerythrocyanin and rod-shaped phycobilisome in cyanobacteria. Molecular Plant **12**, 715-725.

Ho MY, Niedzwiedzki DM, MacGregor-Chatwin C, Gerstenecker G, Hunter CN, Blankenship RE, and Bryant DA. 2019. Extensive remodeling of the photosynthetic apparatus alters energy transfer among photosynthetic complexes when cyanobacteria acclimate to far-red light. Biochimica et Biophysica Acta (BBA)-Bioenergetics, 148064.

Ho MY, Soulier NT, Caniffe DP, Shen G and Bryant DA. 2017. Light regulation of pigment and photosystem biosynthesis in cyanobacteria. Current Opinion in Plant Biology **37**, 24-33.

Ho SH, Liao JF, Chen CY and Chang JS. 2018. Combining light strategies with recycled medium to enhance the economic feasibility of phycocyanin production with *Spirulina platensis*. Bioresource technology **247**, 669-675

Inoue N, Emi T, Yamane Y, Kashino Y, Koike H and Satoh K. 2000. Effects of high-temperature treatments on a thermophilic cyanobacterium *Synechococcus* vulcanus. Plant and Cell Physiology **41**, 515-522.

Jeamton W, Dulsawat S, Tanticharoen M, Vonshak A and Cheevadhanarak S. 2017. Overcoming intrinsic restriction enzyme barriers enhances transformation efficiency in *Arthrospira platensis* C1. Plant and Cell Physiology **58**, 822-830.

Jespersen L, Strømdahl LD, Olsen K and Skibsted LH. 2005. Heat and light stability of three natural blue colorants for use in confectionery and beverages. European Food Research and Technology **220**, 261-266.

Jiang L, Wang Y, Yin Q, Liu G, Liu H, Huang Y and Li B. 2017. Phycocyanin: a potential drug for cancer treatment. Journal of Cancer **8**, 3416-3429.

Kaňa R, Kotabová E, Lukeš M, Papáček Š, Matonoha C, Liu LN, Prášil O, Mullineaux CW. 2014. Phycobilisome mobility and its role in the regulation of light harvesting in red algae. Plant physiology **165**, 1618-1631.

Kannaujiya VK and Sinha RP. 2016. Thermokinetic stability of phycocyanin and phycoerythrin in food-grade preservatives. Journal of Applied Phycology **28**, 1063-1070.

Kannaujiya VK, Kumar D, Pathak J and Sinha RP. 2019. Phycobiliproteins and their commercial significance. In: Mishra AK, Tiwari DN, Rai AN, eds. Cyanobacteria: From Basic Science to Applications. Academic Press, 207-216.

Kannaujiya VK, Sundaram,S. and Sinha RP. 2017. Phycobiliproteins: recent developments and future applications. Singapore: Springer.

Kant R. 2012. Textile dyeing industry an environmental hazard. Natural Science **4**, 22-26.

Khatri A and White M. 2015. Sustainable dyeing technologies. In: Blackburn R ed. Production, Processing and Recycling. Woodhead Publishing, 135-160.

Kumar V, Sonani RR, Shrma M, Gupta GD and Madamwar D. 2016. Crystal structure analysis of C-phycoerythrin from marine cyanobacterium *Phormidium* sp. A09DM. Photosynthesis Research **129**, 17-28.

Kupka M and Scheer H. 2008. Unfolding of C-phycocyanin followed by loss of non-covalent chromophore–protein interactions: 1. Equilibrium experiments. Biochimica et Biophysica Acta **1777**, 94-103.

Lamparter T. 2004. Evolution of cyanobacterial and plant phytochromes. FEBS letters **573**, 1-5.

Leu JY, Lin TH, Sevamani MJP, Chen HC, Liang JZ and Pan KM. 2013. Characterization of a novel thermophilic cyanobacterial strain from Taian hot springs in Taiwan for high CO_2 mitigation and C-phycocyanin extraction. Process Biochemistry **48**, 41-48.

Li D, Wang P, Luo Y, Zhao M and Chen F. 2017. Health benefits of anthocyanins and molecular mechanisms: Update from recent decade. Critical Reviews in Food Science and Nutrition **57**, 1729-1741.

Li W, Pu Y, Ge B, Wang Y, Yu D and Qin S. 2019a. Dye-sensitized solar cells based on natural and artificial phycobiliproteins to capture low light underwater. International Journal of Hydrogen Energy **44**, 1182-1191.

Li W, Su HN, Pu Y, Chen J, Liu LN, Liu Q and Qin S. 2019b. Phycobiliproteins: Molecular structure, production, applications and prospects. Biotechnology Advances **37**, 340-353.

Liang Y, Kaczmarek MB, Kaprzak AK, Tang J, Shah MM R, Jin P, Klepacz-Smółka A, Cheng JJ, Ledakowicz S and Daroch M. 2018. *Thermosynechococcaceae* as a source of thermostable C-phycocyanins: properties and molecular insights. Algal Research **35**, 223-235.

Liang Y, Tang J, Luo Y, Kaczmarek MB, Li X and Daroch M. 2019. *Thermosynechococcus* as a thermophilic photosynthetic microbial cell factory for CO_2 utilisation. Bioresource Technology **278**, 255-265.

Lima GM, Teixeira PC, Texeira CM, Filócomo D and Lage CL. 2018. Influence of spectral light quality on the pigment concentrations and biomass productivity of *Arthrospira platensis*. Algal Research **31**, 157-166.

Liu H, Blankenship RE. 2019. On the interface of light-harvesting antenna complexes and reaction centers in oxygenic photosynthesis. Biochimica et Biophysica Acta (BBA)-Bioenergetics **10**, 148079.

Liu H, Zhang H, Niedzwiedzki DM, Prado M, He G, Gross ML and Blankenship RE. 2013. Phycobilisomes supply excitations to both photosystems in a megacomplex in cyanobacteria. Science **342**, 1104-1107.

Liu LN, Chen XL, Zhng YZ and Zhou BC. 2005. Characterization, structure and function of linker polypeptides in phycobilisomes of cyanobacteria and red algae: an overview. Biochimica et Biophysica Acta **1708**, 133-142.

Liu S, Chen H, Qin S, Zhang W, Guan X and Lu Y. 2009. Highly soluble and stable recombinant holo-phycocyanin alpha subunit expressed in *Escherichia coli*. Biochemical Engineering Journal **1**, 58-64.

Liu S, Chen Y, Lu Y, Chen H, Li F and Qin S. 2010. Biosynthesis of fluorescent cyanobacterial allophycocyanin trimer in *Escherichia coli*. Photosynthesis Research, **105**, 135-142.

Ma Y, Xie J, Zhang C and Zhao J. 2007. Three-stage refolding/unfolding of the dual-color β-subunitin R-phycocyanin from *Polysiphonia urceolata*. Biochemical and Biophysical Research Communications **352**, 787-793.

MacColl R, Eisele LE, Wiliams EC and Bowser SS. 1996. The discovery of a novel R-phycoerythrin from an Antarctic red alga. Journal of Biological Chemistry **271**, 17157-17160.

Madigan M, Bender K, Buckley D, Sattley W and Stahl D. 2018. Brock Biology of Microorganisms, Global 15th Edition. Harlow, United Kingdom: Pearson Education Limited.

Mancini JA, Sheehan M, Kodali G, Chow BY, Bryant DA, Dutton PL and Moser CC. 2018. *De novo* synthetic biliprotein design, assembly and excitation energy transfer. Journal of The Royal Society Interface **15**, 20180021.

Marquardt J, Senger H, Miyashita H, Miyachi S and Mörschel E. 1997. Isolation and characterization of biliprotein aggregates from *Acaryochloris marina*, a Prochloron-like prokaryote containing mainly chlorophyll *d*. FEBS Letters **410**, 428-432.

Martelli G, Folli C, Visai L, Daglia M and Ferrari D. 2014. Thermal stability improvement of blue colorant C-Phycocyanin from *Spirulina platensis* for food industry applications. Process Biochemistry **49**, 154-159.

McCann D, Barrett A, Cooper A, Crumpler D, Dalen L, Grimshaw K, Kitchin E, Lok K, Porteous L, Prince E and Sonuga-Barke E. 2007. Food additives and hyperactive behaviour in 3-year-old and 8/9-year-old children in the community: a randomised, double-blinded, placebo-controlled trial. The Lancet **370**, 1560-1567.

Messerli MA, Amral-Zettler LA, Zettler E, Jung SK, Smith PJ and Sogin ML. 2005. Life at acidic pH imposes an increased energetic cost for a eukaryotic acidophile. Journal of Experimental Biology **208**, 2569-2579.

Miller SR and Castenholz RW. 2000. The evolution of thermotolerance in hot spring cyanobacteria of the genus *Synechococcus*. Journal of Phycology **36**, 48-48.

Minoda A, Sawada H, Suzuki S, Miyashita SI, Inagaki K, Yamamoto T and Tsuzuki M. 2015. Recovery of rare earth elements from the sulfothermophilic red alga *Galdieria sulphuraria* using aqueous acid. Applied Microbiology and Biotechnology **99**, 1513-1519.

Mishra SK, Shrivastav A and Mishra S. 2008. Effect of preservatives for food grade C-PC from *Spirulina platensis*. Process Biochemistry **43**, 339-345.

Mishra SK, Shrivastav A, Pancha I, Jain D and Mishra S. 2010. Effect of preservatives for food grade C-Phycoerythrin, isolated from marine cyanobacteria *Pseudanabaena* sp. International Journal of Biological Macromolecules **47**, 597-602.

Miyagishima S, Wei JL, Nozaki H, Hirooka S. 2017. Cyanidiales: Evolution and Habitats. In: Cyanidioschyzonmerolae. Singapore: Springer, 3-15.

Mogany T, Kumari S, Swalaha FM and Bux F. 2019. Extraction and characterisation of analytical grade C-phycocyanin from *Euhalothece* sp. Journal of Applied Phycology **31**, 1661-1674.

Moldovan S, Ferrandiz M, Franco E, Mira E, Capablanca L and Bonet M. 2017b, October. Printing of cotton with eco-friendly, red algal pigment from *Gracilaria* sp. In IOP Conference Series: Materials Science and Engineering **54**, 192011.

Moldovan S, Ferrandiz MA and Bonet MA. 2017a. Natural cotton printing with red macroalgae biomass of *Gracilaria gracilis* and *Gracilaria cornea*. Annals of the University of Oradea. Fascicle of Textiles, Leatherwork **20**, 61-66.

Moon M, Mishra SK, Kim CW, Suh WI, Park MS and Yang JW. 2014. Isolation and characterization of thermostable phycocyanin from *Galdieria sulphuraria*. Korean Journal of Chemical Engineering **31**, 490-495.

Mullineaux CW, Tobin MJ, Jones GR. 1997. Mobility of photosynthetic complexes in thylakoid membranes. Nature **390**, 421-424.

Niedzwiedzki DM, Liu H and Blankenship RE. 2019. Excitation energy transfer in intact CpcL-phycobilisomes from *Synechocystis* sp. PCC. 6803. The Journal of Physical Chemistry **123**, 4695-4704

Nikolova D, Weber D, Scholz M, Bald T, Scharsack JP and Hippler M. 2017. Temperature-induced remodelling of the photosynthetic machinery tunes photosynthesis in the thermophilic alga *Cyanidioschyzon merolae*. Plant Physiology **174**, 35-46.

Nogami R, Nishida H, Hong DD, Wakisaka M. 2016. Growth promotion of Spirulina by steelmaking slag: application of solubility diagram to understand its mechanism. AMB Express **6**, 1-6.

Ogbonda KH, Aminigo RE and Abu GO. 2007. Influence of temperature and pH on biomass production and protein biosynthesis in a putative *Spirulina* sp. Bioresource Technology **98**, 2207-2211.

Onai K, Morishita M, Itoh S, Okamoto K and Ishiura M. 2004. Circadian rhythms in thethermophilic cyanobacterium *Thermosynechococcus elongatus*: compensation of period length over a wide temperature range. Journal of Bacteriology **186**, 4972-4977.

Pagels F, Guedes A, Amaro HM, Kijjoa A and Vasconcelos V. 2019. Phycobiliproteins from cyanobacteria: Chemistry and biotechnological applications. Biotechnology Advances **37**, 422-443.

Pan-utai W, Kahapana W and Iamtham S. 2018. Extraction of C-phycocyanin from *Arthrospira* (*Spirulina*) and its thermal stability with citric acid. Journal of Applied Phycology **30**, 231-242.

Patel A, Pawar R, Mishra S, Sonawane S and Ghosh PK. 2004. Kinetic studies on thermal denaturation of C-phycocyanin. Indian Journal of Biochemistry and Biophysics **41**, 254-257.

Patel HM, Rastogi RP, Trvedi U and Madamwar D. 2018. Structural characterization and antioxidant potential of phycocyanin from the cyanobacterium *Geitlerinema* sp. H8DM. Algal Research **32**, 372-383.

Pedersen D and Miller SR. 2017. Photosynthetic temperature adaptation during niche diversification of the thermophilic cyanobacterium *Synechococcus* A/B clade. The ISME Journal **11,** 1053.

Petrova N, Todinova S, Laczko-Dobos H, Zakar T, Vajravel S, Taneva S, Gombos Z and Krumova S. 2018. Structural integrity of *Synechocystis* sp. PCC 6803 phycobilisomes evaluated by means of differential scanning calorimetry. Photosynthesis Research **137**, 95-104.

Pittera J, Humily F, Thorel M, Grulois D, Garczarek L and Six C. 2014. Connecting thermal physiology and latitudinal niche partitioning in marine *Synechococcus*. The ISME Journal **8**, 1221-1236.

Pittera J, Partensky F and Six C. 2017. Adaptive thermostability of light-harvesting complexes in marine picocyanobacteria. The ISME Journal **11**, 112-124.

Pradeep HN and Nayak CA. 2019. Enhanced stability of C-phycocyanin colorant by extrusion encapsulation. Journal of Food Science and Technology **56** ,1-9.

Rahman DY, Sarian FD, Va Wijk A, Martinez-Garcia M and Van der Maarel MJ EC. 2017. Thermostable phycocyanin from the red microalga *Cyanidioschyzon merolae*, a new natural blue food colorant. Journal of Applied Phycology **29**, 1233-1239.

Rast A, Schaffer M, Albert S, Wan W, Pfeffer S, Beck F, Plitzko JM, Nickelsen J and Engel BD. 2019. Biogenic regions of cyanobacterial thylakoids form contact sites with the plasma membrane. Nature Plants **5**, 436-446.

Reddy A, Norris DF, Moeni SS, Waldo B and Ruby JD. 2016. The pH of beverages available to the American consumer. Journal of the American Dental Association **147**, 255-263.

Reisser W. 2013. Polyextremophilic Photoautotrophic Eukaryotic Algae. In Seckbach J, Oren A, Stan-Lotter H, eds. Polyextremophiles. Cellular Origin, Life in Extreme Habitats and Astrobiology. Dordrecht: Springer, 567-580.

Research and Markets. 2019. Natural food colors market by form, by application, by region; size and forecast, 2015-2025 (https://www.researchandmarkets.com/research/7kwgvv).

Rossoni AW and Weber AP. 2019. Systems biology of cold adaptation in the polyextremophilic red alga *Galdieria sulphuraria*. Frontiers in Microbiology **10**, 927.

Ruan Z, Prášil O and Giordano M. 2018. The phycobilisomes of *Synechococcus* sp. are constructed to minimize nitrogen use in nitrogen-limited cells and to maximize energy capture in energy-limited cells. Environmental and Experimental Botany **150**, 152-160.

Saer RG and Blankenship RE. 2017. Light harvesting in phototrophic bacteria: structure and function. Biochemical Journal **474**, 2107-2131.

Samsonoff WA and MacColl,R. 2001. Biliproteins and phycobilisomes from cyanobacteria and red algae at the extremes of habitat. Archives of Microbiology **176**, 400-405.

Sarada R, Pillai MG and Ravishankar GA. 1999. Phycocyanin from *Spirulina* sp: influence of processing of biomass on phycocyanin yield, analysis of efficacy of extraction methods and stability studies on phycocyanin. Process Biochemistry **34**, 795-801.

Scheer H and Zhao KH. 2008. Biliprotein maturation: the chromophore attachment. Molecular Microbiology **68**, 263-276.

Schrantz K, Wyss PP, Ihsen J, Toth R, Bora DK, Vitol EA, Rozhkova EA, Pieles U, Thöny-Meyer L and Braun A. 2017. Hematite photoanode co-functionalized with self-assembling melanin and C-phycocyanin for solar water splitting at neutral pH. Catalysis Today **284**, 44-51.

Seckbach J. 2005. The Relevance of Halophiles and other Extremophiles to Martian and Extraterrestrial Environments. In: Gunde-Cimerman N, Oren A, Plemenitaš A, eds. Adaptation to Life at High Salt Concentrations in Archaea, Bacteria, and Eukarya. Cellular Origin, Life in Extreme Habitats and Astrobiology. Dordrecht: Springer, 123-136.

Selig MJ, Malchione NM, Gamaleldin S, Padilla-Zakour OI and Abbaspourrad A. 2018. Protection of blue color in a spirulina derived phycocyanin extract from proteolytic and thermal degradation via complexation with beet-pectin. Food Hydrocolloids **74**, 46-52.

Sharma K, Sharma V and Sharma SS. 2018. Dye-sensitized solar cells: fundamentals and current status. Nanoscale Research Letters **13**, 381.

Sheehan MM, Magaraci MS, Kuznetsov IA, Mancini JA, Kodali G, Moser CC, Dutton PL and Chow BY. 2018. Rational construction of compact *de novo*-designed biliverdin-binding proteins. Biochemistry **57**, 6752-6756.

Shiraishi H and Tabuse, Y. 2013. The AplI restriction-modification system in an edible cyanobacterium, *Arhrospira* (*Spirulina*) *platensis* NIES-39, recognizes the nucleotide sequence 5′-CTGCAG-3′. Bioscience, Biotechnology and Biochemistry **77**, 782-788.

Six C, Thomas JC, Gaczarek L, Ostrowski M, Dufresne A, Blot N, Scanlan DJ, and Partensky F. 2007. Diversity and evolution of phycobilisomes in marine *Synechococcus* sp: a comparative genomics study. Genome Biology doi: 10.1186/gb-2007-8-12-r259.

Spolaore P, Joannis-Cassan C, Duran E and Isambert A. 2006. Commercial applications of microalgae. Journal of Bioscience and Bioengineering **101**, 87-96.

Stoitchkova K, Zsiros O, Jávorfi T, Páli T, Andreeva A, Gombos Z and Garab G. 2007. Heat-and light-induced reorganizations in the phycobilisome antenna of *Synechocystis* sp. PCC 6803. Thermo-optic effect. Biochimica et Biophysica Acta **1767**, 750-756.

Sumiya N, Fujiwara T, Kobayashi Y, Misumi O, Miyagishima SY. 2014. Development of a heat-shock inducible gene expression system in the red alga *Cyanidioschyzon merolae*. PLoS One doi: 10.1371/journal.pone.0111261.

Sun L, Wang S and Qiao Z. 2006. Chemical stabilization of the phycocyanin from cyanobacterium *Spirulina platensis*. Journal of Biotechnology **121**, 563-569.

Tooley AJ, Cai YA and Glazer AN. 2001. Biosynthesis of a fluorescent cyanobacterial C-phycocyanin holo-α subunit in a heterologous host. Proceedings of the National Academy of Sciences of The United States of America **98**, 10560-10565.

Toong C. 2018. Understanding the thermal stability and environmental sensitivity of phycocyanin using spectroscopic and modelling tools. Masters Thesis, University of Massachusets.

Tragut V, Xiao J, Bylina EJ and Borthakur D. 1995. Characterization of DNA restriction-modification systems in *Spirulina platensis* strain pacifica. Journal of Applied Phycology **7**, 561-564.

Vasudevan R, Gale GA, Schiavon AA, Puzorjov A, Malin J, Gillespie MD, Vavitsas K, Zulkower V, Wang B, Howe CJ, Lea-Smith DJ and McCormick AJ. 2019. CyanoGate: A modular cloning suite for engineering cyanobacteria based on the plant MoClo syntax. Plant Physiology **180**, 39-55.

Vásquez-Suárez A, Lobos-González F, Cronshaw A, Sepúlveda-Ugarte J, Figueroa M, Dagnino-Leone J, Bunster M and Martínez-Oyanedel J. 2018. The γ33 subunit of R-phycoerythrin from *Gracilaria chilensis* has a typical double linked phycourobilin similar to γ subunit. PloS One doi: 10.1371/journal.pone.0195656..

Wagner JR, Zhang J, Brunzelle JS, Vierstra RD, Forest KT. 2007. High resolution structure of Deinococcus bacteriophytochrome yields new insights into phytochrome architecture and evolution. Journal of Biological Chemistry **282**, 12298-12309.

Wall KP, Dillon R and Knowles MK. 2015. Fluorescence quantum yield measurements of fluorescentproteins: a laboratory experiment for a biochemistry or molecular biophysics laboratory course. Biochemistry and Molecular Biology Education **43**, 52-59.

Wan M, Wang Z, Zhang Z, Wang J, Li S, Yu A, Li Y. 2016. A novel paradigm for the high-efficient production of phycocyanin from *Galdieria sulphuraria*. Bioresource technology **218**, 272-278.

Watanabe M, Semchonok DA, Webber-Birungi MT, Ehira S, Kondo K, Narikawa R, Ohmori M, Boekema EJ and Ikeuchi M. 2014. Attachment of phycobilisomes in an antenna-photosystem I supercomplex of cyanobacteria. Proceedings of the National Academy of Sciences of The United States of America **111**, 2512-2517.

Weber A, Oesterhelt C, Gross W, Bräutigam A, Imboden L, Krassovskaya I, Linka N, Truchina J, Schneidereit J, Voll H and Voll L. 2004. EST-analysis of the thermo-acidophilic red microalga *Galdieria sulphuraria* reveals potential for lipid A biosynthesis and unveils the pathway of carbon export from rhodoplasts. Plant Molecular Biology **55**, 17-32.

Włodarczyk A, Selão TT, Noling B and Nixon PJ. 2019. Unprecedented biomass and fatty acid production by the newly discovered cyanobacterium *Synechococcus* sp. PCC 11901. BioRxiv doi: 10.1101/684944.

Wu HL, Wang GH, Xiang WZ, Li T and He H. 2016. Stability and antioxidant activity of food-grade phycocyanin isolated from *Spirulina platensis*. International Journal of Food Properties **19**, 2349-2362.

Yamanaka G and Glazer AN. 1980. Dynamic aspects of phycobilisome structure. Archives of Microbiology **124**, 39-47.

Yan M, Liu B, Jiao X and Qin S. 2014. Preparation of phycocyanin microcapsules and its properties. Food and Bioproducts Processing **92**, 89-97.

Yang P, Li B, Yin QF, and Wang YJ. 2017. Carboxymethyl chitosan nanoparticles coupled with CD59-specific ligand peptide for targeted delivery of C-phycocyanin to HeLa cells. Tumor Biology doi: 10.1177/1010428317692267.

Zhang J, Ma J, Liu D, Qin S, Sun S, Zhao J and Sui SF. 2017. Structure of phycobilisome from the red alga *Griffithsia pacifica*. Nature **551**, 57.

Zhao KH, Deng MG, Zheng M, Zhou M, Parbel A, Storf M, Meyer M, Strohmann B and Scheer H. 2000. Novel activity of a phycobiliprotein lyase: both the attachment of phycocyanobilin and the isomerization to phycoviolobilin are catalyzed by the proteins PecE and PecF encoded by the phycoerythrocyanin operon. FEBS letters 469, 9-13.

Zhao KH, Wu D, Zhang L, Zhou M, Böhm S, Bubenzer C and Scheer H. 2006. Chromophore attachment in phycocyanin. Functional amino acids of phycocyanobilin–α-phycocyanin lyase and evidence for chromophore binding. The FEBS Journal **273**, 1262-1274.

Zhao KH, Zhu JP, Deng MG, Zhou M, Storf M, Parbel A and Scheer H. 2003. Photochromic chromopeptides derived from phycoerythrocyanin: biophysical and biochemical characterization. Photochemical and Photobiological Sciences **2**, 741-74.

Figure legends

Figure 1. Key components and structures of a phycobilisome complex. (A) Molecular structure of phycocyanin α- and β-subunits from *T. vulcanus* (PDB ID: 3O18), with α-helices labelled (A-I for the α-subunit and A-J for the β-subunit). The bilin chromophores (one for the α-subunit and two for the β-subunit) are shown in green. (B) Biosynthesis pathway of bilin chromophores from heme to biliverdin IXα (BV) to phycocyanin (PCB), phycoerythrobilin (PEB), phycoviolobilin (PVB) and phycourobilin (PUB). Enzymes written in blue are heme oxygenase (HO), phycocyanobilin:ferredoxin oxidoreductase (PcyA), 15,16-dihydrobiliverdin:ferredoxin oxidoreductase (PebA), phycoerythrobilin:ferredoxin oxidoreductase (PebB) and two lyases-isomerases (PecE/PecF and RpcG). The structural differences between linear tetrapyrroles relative to PCB are highlighted with red. The approximate colour of individual bilin chromophores is shown when attached to the PC α-subunit of *Synechocystis* sp. PCC 6803 following heterologous production in *E. coli* (Alvey et al., 2011). Lyases required for the attachment of PCB and PEB to their cognate apo-proteins (indicated here by the Cys-binding site) are not shown. (C) Schematic structures of the hemi-discoidal phycobilisomes in *T. vulcanus* (left) (Nganou et al., 2016) and *Synechocystis* sp. PCC 6803 (middle), and the rod-shaped phycobilisome from *Leptolyngbya* sp. PCC 6406 that attaches to photosystem I (PSI) via linker peptide CpcL (right) (Hirose et al., 2019). Evidence suggests that hemi-discoidal phycobilisomes can attach to photosystem II (PSII) or PSI (Arteni et al., 2009; Liu et al., 2013). Abbreviations: APC, allophycocyanin; PC, phycocyanin; PE, phycoerythrin.

Figure 2. Comparison of the phycocyanin α-subunit peptide sequences of cyanobacteria that grow in different environments. The predicted average flexibility of amino acids are shown for different habitat classes including hyperthermophiles, thermophiles, thermoacidophiles, mesophiles, and cold-adapted species (as in **Table 1**). Flexibility values were calculated using the Expasy tool ProtScale (average flexibility scale, window size 9) (Gasteiger et al., 2005). The average flexibility for hypethermophiles was shifted two residues to the right starting from position 74 to account for a common truncation (position 74 and 75). A multiple sequence alignment is shown for species described in this study (generated using T-Coffee, EMBL-EBI), including hyperthermophiles (dark red), thermophiles (light red), thermoacidophiles (orange), mesophiles (green) and cold-adapted species (blue) (UniProt IDs: U3SBH4, W0FL73, Q85G43,A0A1L6BXH4, P50032, Q54715, P00306, P72509,

A0A2D2Q3Q2, Q9AM02, Q2JT28, A0A1L6BXJ3). Incomplete sequences for *Synechococcus* OH28 and OH20 are marked with asterisks. Due to the unavailability of complete sequences for *Synechococcus* OH28 and OH20, the full sequence of *Synechococcus* sp. JA-3-3Ab was added for comparison (100% identity match with *Synechococcus* OH20 based on the available sequence). Alignments were coloured using the Clustal X colour scheme (www.clustal.org). The predicted locations of α-helices are taken from the crystal structure of *T. vulcanus* (PDB ID: 3O18), and are labelled in light red. The phycocyanobilin binding site (C84) is labelled in blue (PCB). The key amino acid substitutions that are predicted to contribute to thermostability are marked based on study in red (Liang et al., 2018), blue (Pittera et al., 2017), green (Rahman et al., 2017) or dark grey arrows (identified here based on the average flexibility analysis).

Figure 3. Molecular structure of phycocyanin showing key amino acid substitutions that could influence thermostability. (A) Top view of the structure of the $(\alpha\beta)_6$ PC hexamer from *A. platensis* (PDB ID: 1GH0). The locations of three hot spots that contribute to thermostability are marked with black rectangles (Liang et al., 2018). (B) A side-view of the $(\alpha\beta)_6$ hexamer from *A. platensis* showing the top and bottom $(\alpha\beta)_3$ trimer, (C and D) The structure of a single hot spot within the $(\alpha\beta)_6$ hexamer from (C) *A. platensis* or (D) *T. elongatus* (PDB ID: 3L0F). The residues of α-helix B from two PC α-subunits located in the top and bottom $(\alpha\beta)_3$ trimer within the $(\alpha\beta)_6$ hexamer (i.e. one of the three hot spots) are shown in cartoon. The key residues at the positions 21, 28, 33, 37, 42, 43 and 145 highlighted by Liang et al. (2018) are shown in sticks, labelled and highlighted with either orange or green for the bottom or top $(\alpha\beta)_3$ trimer, respectively. Polar interactions (i.e. hydrogen bonds and salt bridges) for key residues are shown in magenta for the bottom $(\alpha\beta)_3$ trimer or cyan for the top $(\alpha\beta)_3$ trimer. More specific details for residue interactions are described in Liang et al. (2018).

Table 1. Growth conditions for cyanobacteria and red algae species from different habitats. The recorded minimum temperature for growth (T_{min}), optimal temperature for growth (T_{opt}) and maximum temperature for growth (T_{max}) are shown. Hyperthermophilic, thermophilic (or thermoacidophilic) and mesophilic species have optimal growth temperature above 60, 40 and 15 °C, respectively. In contrast to mesophiles, cold-adapted species are able to tolerate temperatures below 15 °C (with optimal growth temperature at *ca*. 20 °C).

Type	**Species**	**T_{min}**	**T_{opt}**	**T_{max}**	**References**
Hyperthermophile	*Synechococcus* sp. JA-3-3Ab	40	55	65	Allewalt et al. (2006)
	Synechococcus sp. OH20	50	57	62	Miller and Castenholz (2000); Pedersen and Miller (2017)
	Synechococcus sp. OH28	50	65	70	Miller and Castenholz (2000); Pedersen and Miller (2017)
Thermophile	*Thermosynechococcus elongatus* BP-1	30	45-55	55	Onai et al. (2004); Liang et al. (2018)
	Thermosynechococcus elongatus PKUAC-SCTE542	45	55	60	Liang et al. (2019)
	Thermosynechococcus vulcanus NIES 2134	30	50	55	Onai et al. (2004); Liang et al. (2018)
	Synechococcus lividus PCC 6715	-	50	55	Liang et al. (2018)
Thermoacidophile	*Galdieria sulphuraria*	25	40-50	56	Hirooka and Miyagishima (2016); Rossoni and Weber (2019)
	Cyanidioschyzon merolae	25	40-45	50	Sumiya et al. (2014); Nikolova et al. (2017)
Mesophile	*Synechocystis* PCC 6803	25	30	40	Inoue et al. (2001)
	Arthrospira platensis	20	35	40	Kumar et al. (2011)
	Synechococcus M16.1	18	32	35	Pittera et al. (2017)
Cold-adapted	*Synechococcus* MVIR-18-1	10	22	25	Pittera et al. (2017)

Table 2. Studies investigating the effect of additives or genetic modifications on the stability of phycobiliproteins or phycobilisomes from different mesophilic species. The ranges of temperatures, pH, buffers and incubation conditions under which phycobilisomes (PBPs) or phycobiliproteins (PCBs) were tested are indicated where available. Buffer abbreviations: AB, acetate buffer; CP, citrate phosphate; PB, phosphate buffer; SGF, simulated gastric fluid; SIF, simulated intestinal fluid. Methods abbreviations: ABS, absorbance spectroscopy; AOA, antioxidant activity; CD, circular dichroism; DLS, dynamic light scattering; DOR, dynamic oscillatory rheology; DSC, differential scanning calorimetry; DU, denaturation with urea; FAN, fluorescence anisotropy; FS, fluorescence spectroscopy; KS, kinetics study; LAB, CIELAB colour space; PD, proteolytic digestion; PHB, photobleaching; V, viscometry. Additives abbreviations: AS, ascorbic acid; BA, benzoic acid; BEP, beet pectin; CA, citric acid; DSP, dithiobis(succinimidyl propionate); FA, formaldehyde; FRU, fructose; GA, gluteraldehyde; GAR, gum arabic (primarily arabinogalactan); GG, guar gum; GLU, glucose; GLY, glycerol; hisMBP, his6-maltose-binding protein; LAC, lactose; MAL, maltose; MGO, methylglyoxal; MH, manuka-honey; PEO, polyethylene oxide; SAL, sodium alginate; SDS, sodium dodecyl sulphate; SOA, sorbic acid; SOR, sorbitol; SSPS, soluble soy polysaccharides; SUC, sucrose.

Source organism	**PBS/PBP**	**Temperatures (°C)**	**pH and buffers**	**Additive or modification**	**Testing methodology**	**References**
Arthrospira platensis	PBS	30-180	4.5, 7.0 and 9.0 in Tris–HCl (100 mM)	$CaCl_2$ (4, 20 mM), SUC (30%, 50% [w/v])	ABS, DSC, DOR, V	Chronakis (2001)
		-	7.0 in PB (500 mM)	DSP	ABS, FS, UD (4 M for 8-hour)	Fukui et al. (2004)
		45, 50 and 55	Microencapsulation using SAL (0.7-2.1% w/w) and chitosan (0.5-3.0% w/w)	GAR	KS, ABS measured after 5-hour incubation, PHB	Jespersen et al. (2005)
		60 and 100	7.0 in PB (50 mM)	FA (2.5% [v/v])	SDS-PAGE after incubation for 10 minutes or 3 hours	Sun et al. (2006)
		50-65	5.0 in AB (10 mM), 6.0-7.0 in PB (10 mM)	SOR (10-50% [w/w])	KS, ABS during 30-min incubation	Antelo et al. (2008)

0 and 35, 20-80	7.0 in PB (0.1 M)	CA, SUC, $CaCl_2$ (all 4 mg/ml)	ABS measured during 45-day incubation, DSC, DU (0-10.0 M)	Mishra et al. (2008)
4, 26-75	5.0-7.0 in CP	GLU (0-40% [w/v]), SUC (0-40% [w/v]), SOR (200 mg/ml), NaCl (0-40% [w/v]), AA (4 mg/ml), SA (4 mg/ml), NaN_3 (0.5 mg/ml)	KS, ABS measured during 30-min, 4-hour or 120-day incubation	Chaiklahan et al. (2012)
25-100	7.2 in PB (0.1 M)	MGO, MH (80% [w/v]), FRU (62% [w/v]), GLU (37% [w/v]), SUC (54% [w/v]), LAC (14% [w/v]), MAL (42% [w/v])	ABS measured after 30-min incubation	Martelli et al. (2014)
25, 40 and 50	7.0 in PB (0.1 M) 1.2 in SGA (0.1-0.15 M), 7.4 in SIF (~70 mM)	Microencapsulation using SAL (0.7-2.1% [w/w]) and chitosan (0.5-3.0% [w/w])	ABS measured during 40-day incubation	Yan et al. (2014)
25-75	3.0-8.0 in CP (50 mM)	SUC, GLU, NaCl (all 20% [w/v])	KS, ABS measured during 30-min incubation, PHB	Wu et al. (2016)
55-75	6.5 in water with 20% ZSM	PEO nanofibers (6% [w/v]), SUC (20% [w/v]), GLU (20% [w/v]), NaCl (2.5% [w/v]), SOR (50% [w/v])	KS, ABS	Braga et al. (2016)
-	1.9-7.0 in CP (~40 mM)	SDS (0-1.1% [w/w])	ABS, LAB	Falkeborg et al. (2018)
40, 60 and 80	6.0 in CP (0.1 M)	GLU, FRU , SUC (all 10 and 15% [w/w])	KS, ABS measured during 60-min incubation, LAB and AOA measured after 60-min incubation	Hadiyanto et al. (2018)
40 and 80	6.0-7.0 in water	GLY (0, 40% and 100% [v/v])	KS, FS measured during 60-min incubation, FAN	Toong et al. (2018)
40, 50, 65, 80 and 90	6.8 in CP (50 mM)	BEP, GG, SSPS (all 2% [w/w])	LAB measured after 20 or 45-min incubation, PD	Selig et al. (2018)

		80	7.0 in PB (0.1 M)	CA (4 mg/ml)	ABS measured during 60-min incubation	Pan-utai et al. (2018)
		40-80	4.5-7.0 in PB	Microencapsulation using SAL (1.5-2.5% [w/v])	ABS measured during 2-hour incubation	Pradeep and Nayak (2019)
Callithamnion rubosum	R-PE	5-90	5.7 in MES buffer (10 mM), water	CdS nanoparticles	ABS, CD	Bekasova et al. (2013)
	R-PE	15-90	water	Ag^0 nanoparticles	ABS, FS, CD, DLS	Bekasova et al. (2016)
Porphyridium cruentum	B-PE	4 and 25, 20-95	1.1-13.6 in PB (20 mM)	SUC, NaCl (all 4 mg/ml);	ABS, FS, CD, PHB measured during 18-day incubation	González-Ramírez et al. (2014)
	PBS	RT	6.8-7.5 in PB (0.75-750 mM)	FA, GA, SUC (1 M)	ABS, FS	Cubicciotti (1997)
Synechocystis sp. PCC 6803	C-PC (□-subunit)	4 and 25	5.5-6.5 in MES-KOH (25 mM), 6.5-7.5 in MOPS-KOH (25 mM), 7.4 in PB (50 mM), 7.5-8.5 in Tris-HCl (25 mM), 8.5-10.0 in glycine-KOH (25 mM)	HisMBP fusion tag	ABS, FS measured during 5-day incubation, PHB	Liu et al. (2009)
	PBS (*in vivo*, *in vitro*)	20-120	7.0 in PB (0.75 M)	SUC (0.5-0.75 M)	ABS, DSC	Petrova et al (2018)
Pseudanabaena sp.	C-PE	0 and 35	7.2 in PB (0.1 M), 2.0-12.0 in PB (50 mM)	CA, SUC, $CaCl_2$ (all 4 mg/ml)	ABS measured during 45-day incubation	Mishra et al. (2010)
Nostoc sp. HKAR-2	PC; PE	4, 25 and 40	7.0 in PB (50 mM)	BA, CA, SUC, AA, $CaCl_2$ (all 0.5-5 mM)	KS, ABS measuring during 30-day incubation	Kannaujiya and Sinha (2016)
Euhalothece sp.	PBS	4 and 25, 25-65	4.0-9.0 in PB (100 mM)	Citric acid (0.4% [w/v]), NaN3 (0.005% [w/v]) with EDTA (1 mM), NaCl (20% [w/v])	ABS and AOA measured after 2-hour or during 24-hour and 42-day incubation	Mogany et al. (2019)

A

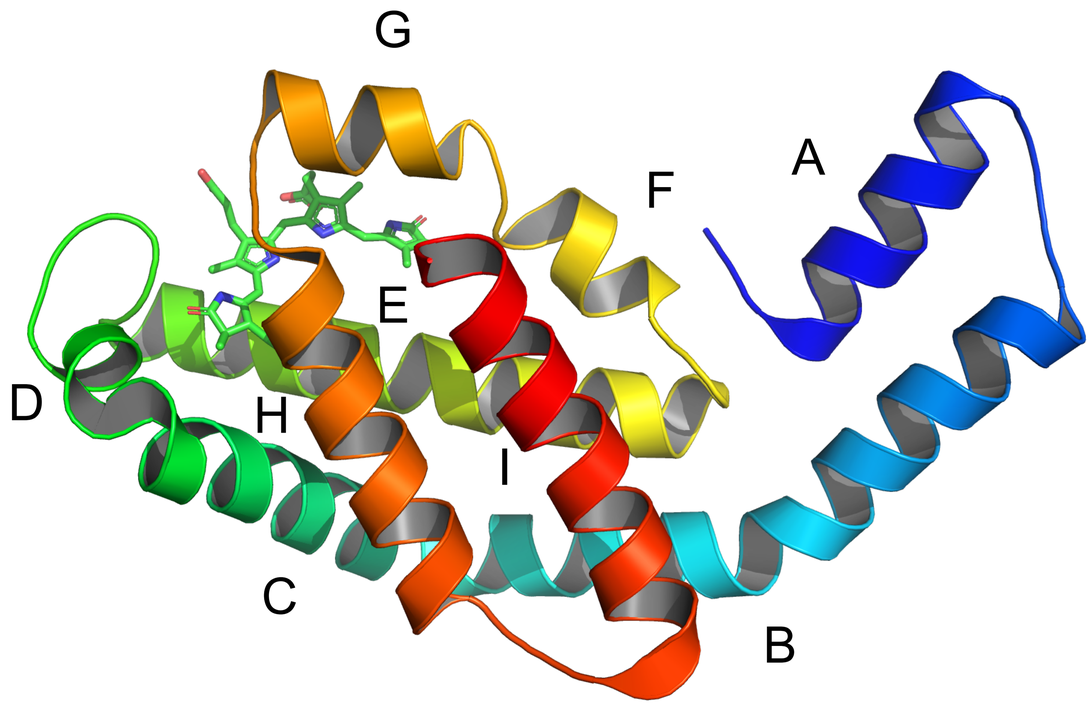

PC α-subunit

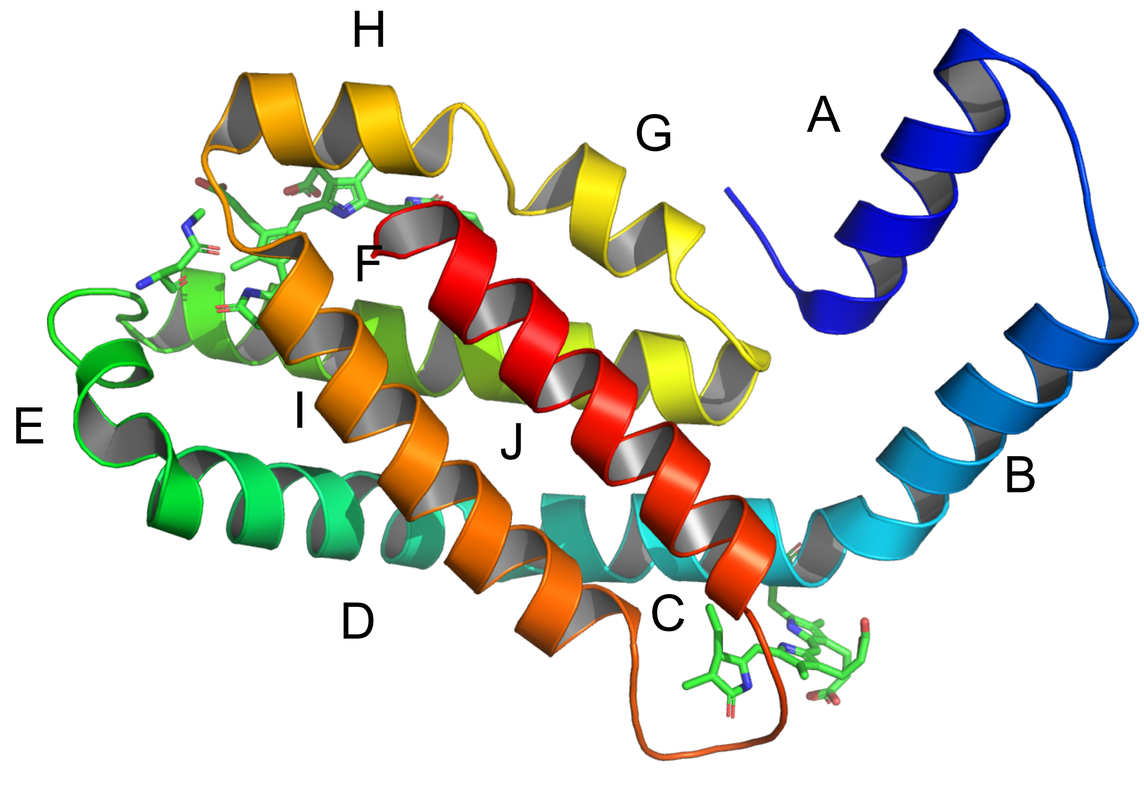

PC β-subunit

B

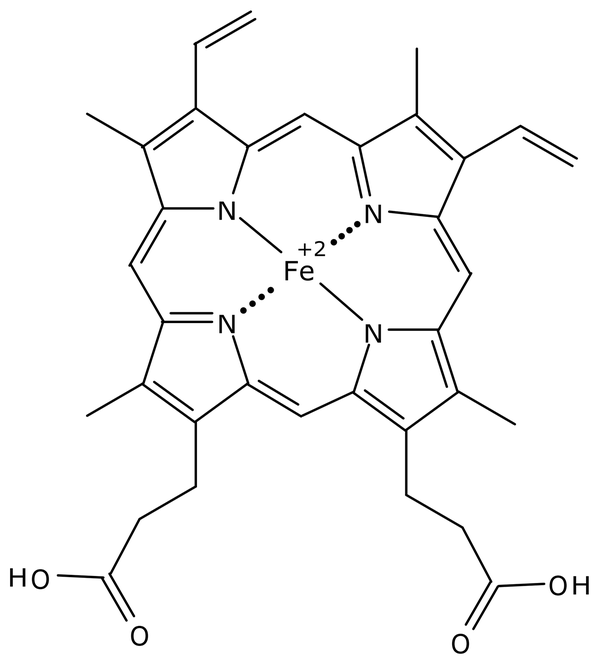

Heme

HO

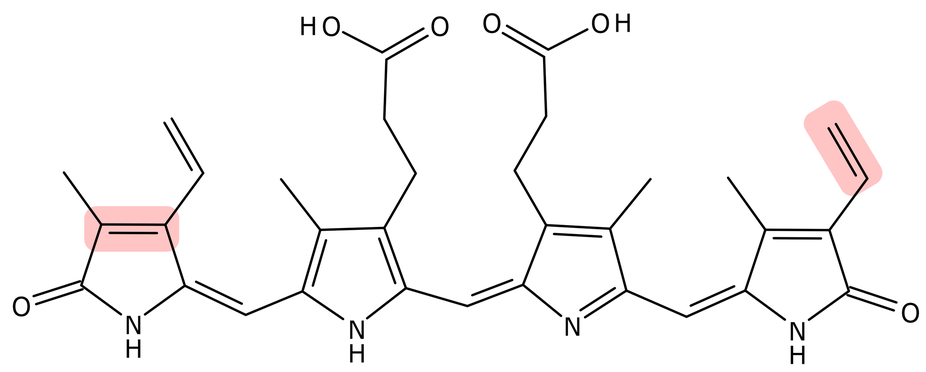

Biliverdin IXα (BV)

PcyA

PebA/PebB

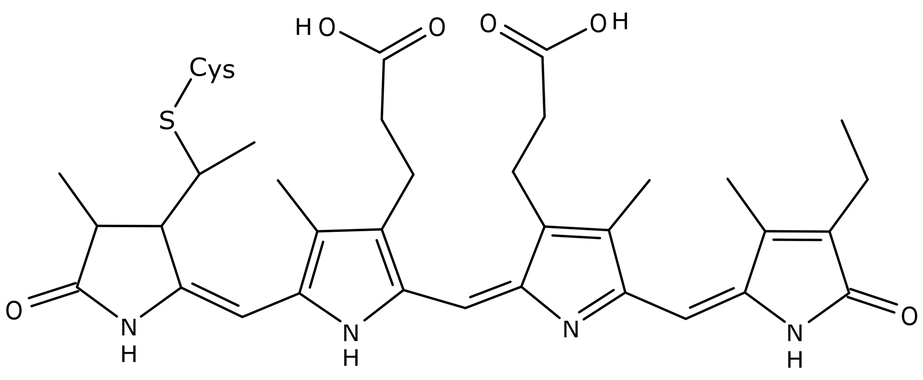

Phycocyanobilin (PCB)

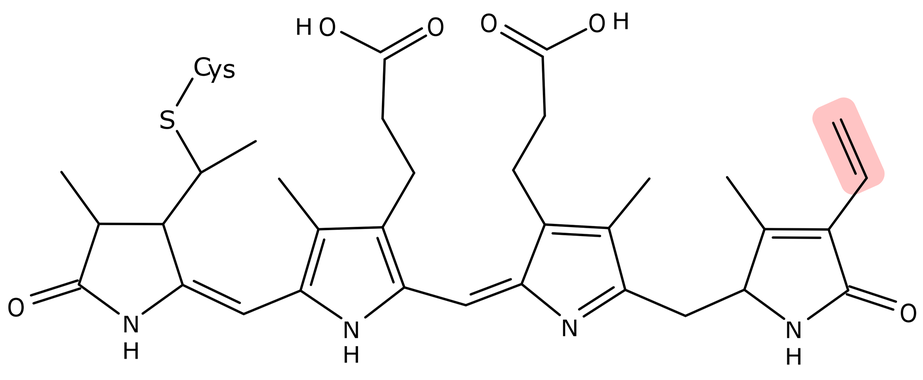

Phycoerythrobilin (PEB)

PecE/PecF

RpcG

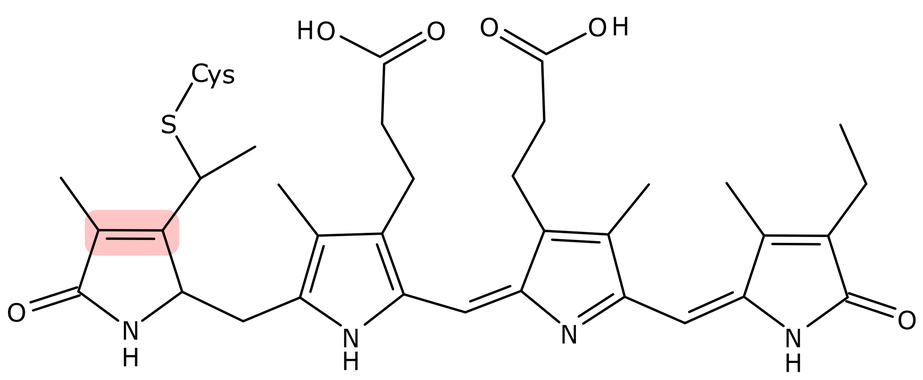

Phycoviolobilin (PVB)

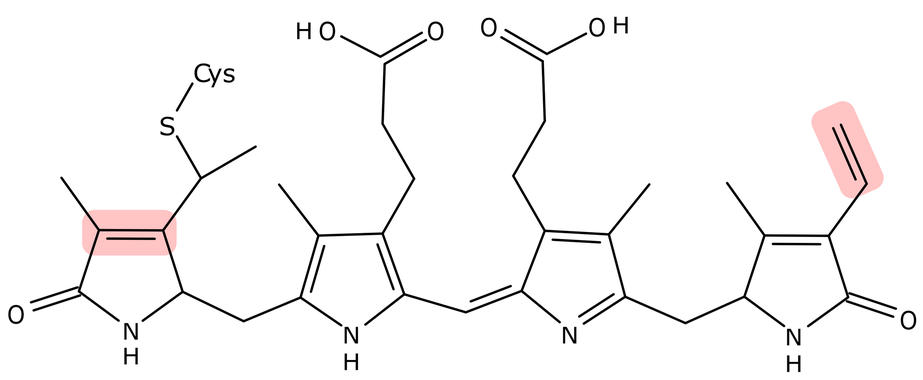

Phycourobilin (PUB)

C

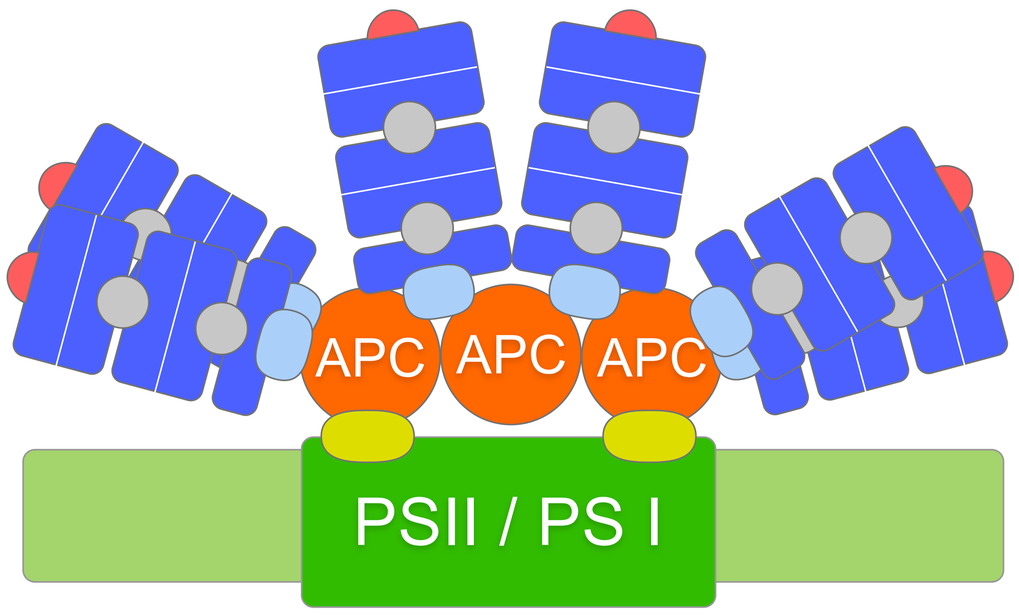

D

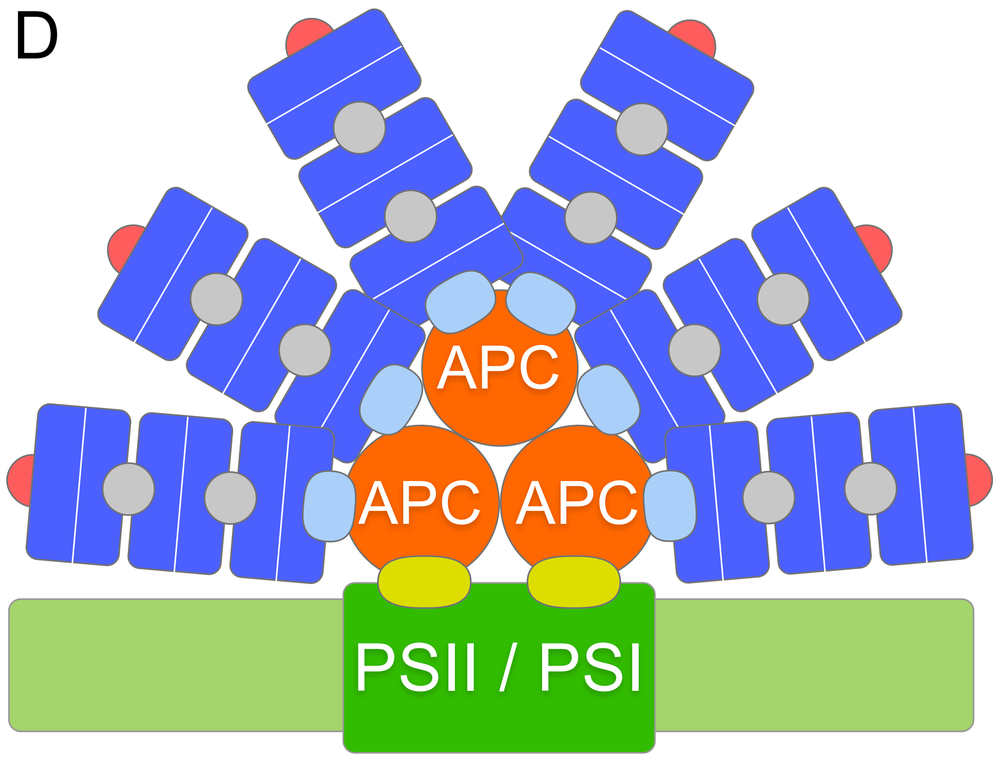

E

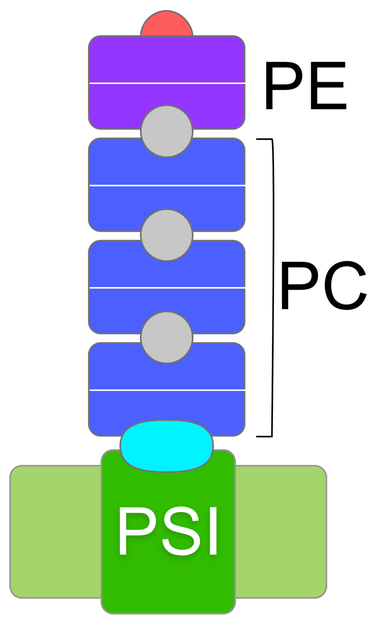

core-membrane linker core-rod linker rod linker rod capping linker CpcL

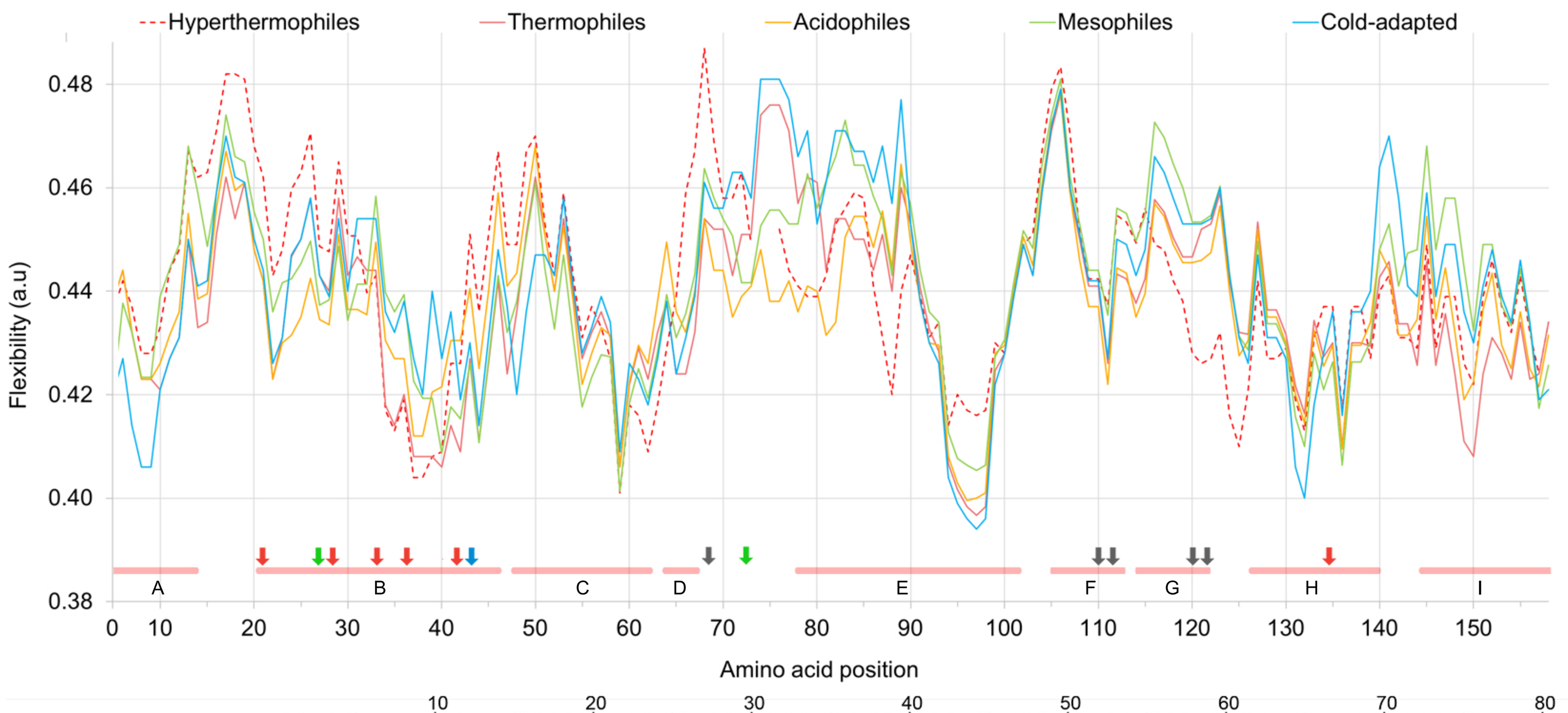
Hyperthermophiles
Thermophiles
Acidophiles
Mesophiles
Cold-adapted
Flexibility (a.u)
0.48
0.46
0.44
0.42
0.40
0.38
A
B
C
D
E
F
G
H
I
0 10 20 30 40 50 60 70 80 90 100 110 120 130 140 150
Amino acid position
10 20 30 40 50 60 70 80
Synechococcus sp. JA-3-3Ab MQTPIVDAIATADSQGRYLSNSELQAINGRFQRAAASMEAARVLSSRAEELVRGATEAVYAKFPYTTQPGGQC--HTQAGK
Synechococcus sp. OH20 MQTPIVDAIATADSQGRYLSNSELQAINGRFQRAAASMEAARVLSSRAEELVRGATEAVYAKFPYTTQPGGQC--HTQAGK
Synechococcus sp. OH28 MQTPIVDAIATADSQGRYLSNSELQAISGRFQRAAASMEAARVLSSRAEELVRGATEAVYAKFPYTTQPGGQC--HTQAGK
T. elongatus BP-1 MKTPITEAIAAADTQGRFLSNTELQAVDGRFKRAVASMEAARALTNNAQSLIDGAAQAVYQKFPYTTTMQGSQYASTPEGK
T. vulcanus MKTPITEAIAAADTQGRFLSNTELQAVDGRFKRAVASMEAARALTNNAQSLIDGAAQAVYQKFPYTTTMQGSQYASTPEGK
S. lividus PCC 6715 MKTPITEAIAAADTQGRFLSNTELQAADGRFKRAVASMEAARALTNNAQSLIDGAAQAVYQKFPYTTTMQGSQYASTPEGK
G. sulphuraria MKTPITEAIAAADNQGRFLSNTELQAVNGRYQRAAASLEAARSLTSNAERLINGAAQAVYSKFPYTSQMPGPQYASSAVGK
C. merolae 10D MKTPITEAIAAADSQGRFLSNTELQACFGRFQRAAASLEAARALTSNAQRLIDGAANAVYSKFPYTTQMTGACYASSAVGK
Synechocystis sp. PCC 6803 MKTPLTEAVSTADSQGRFLSSTELQIAFGRLRQANAGLQAAKALTDNAQSLVNGAAQAVYNKFPYTTQTQGNNFAADQRGK
A. platensis MKTPLTEAVSIADSQGRFLSSTEIQVAFGRFRQAKAGLEAAKALTSKADSLISGAAQAVYNKFPYTTQMQGPNYAADQRGK
Synechococcus sp. M16.1 MKTPLTEAVAAADSQGRFLSNTEVQAASGRFNRAKASLEAAKALTSKADSLVNGAAQAVYTKFPYTTQMEGSNYSATAEGK
Synechococcus sp. MVIR-18-1 MKTPLTEAVAAADSQGRFLSNTEVQAASGRFNRAQASLEAAKGLTAKADSLVSGATQAVYTKFPYTTQMEGPNYSTTPEGK
α-helix
A
B
C
D
E
PCB
90 100 110 120 130 140 150 160
Synechococcus sp. JA-3-3Ab DKCARDVRHYLRYITYCLVAGGTGPLDEYQLAGIREINAAFELSPSWFIEALRYIKANHGLTGQAATEANTYIDYAINALS
Synechococcus sp. OH20 DKCARDVRHYLRYITYCLVAGGTGPLDEYQLAGIREIN*
Synechococcus sp. OH28 DKCARDVRHYLRYITYCLVAGGTGPLDECMLAGIREIN*
T. elongatus BP-1 AKCARDIGYYLRMVTYCLVAGGTGPMDEYLIAGLSEINSTFDLSPSWYIEALKYIKANHGLTGQAAVEANAYIDYAINALS
T. vulcanus AKCARDIGYYLRMITYCLVAGGTGPMDEYLIAGLSEINSTFDLSPSWYIEALKYIKANHGLTGQAAVEANAYIDYAINALS
S. lividus PCC 6715 AKCARDIGYYLRMVTYCLVAGGTGPMDEYLIAGLAEINSTFDLSPSWYVEALKYIKANHGLSGQAAVEANAYIDYAINALS
G. sulphuraria AKCARDIGYYLRMVTYCLVVGGTGPMDEYLIAGLEEINRTFDLSPSWYVEALNYIKANHGLSGQAANEANTYIDYAINALS
C. merolae 10D AKCSRDVGYYLRMITYCLVAGGTGPMDEYLVAGLDEVNRAFDLSPSWYIEALKYIKANHGLSGAAASEANAYINYAINALS
Synechocystis sp. PCC 6803 DKCARDIGYYLRIVTYCLVAGGTGPLDEYLIAGIDEINRTFDLSPSWYVEALKYIKANHGLSGDARDEANSYLDYAINALS
A. platensis DKCARDIGYYLRMVTYCLIAGGTGPMDEYLIAGIDEINRTFELSPSWYIEALKYIKANHGLSGDAATEANSYLDYAINALS
Synechococcus sp. M16.1 AKCSRDVGYYLRMITYCLVAGGTGPMDDYLIAGLDEINRTFELSPSWYVEALKHIKANHGLSGDAATEANSYIDYAINALI
Synechococcus sp. MVIR-18-1 AKCSRDIGYYLRMVTYCLVAGGTGPMDDYLIAGLDEINRTFELSPSWYVEALKHIKSNHGLSGDAATEANSYINYAINALT
α-helix
E
F
G
H
I
Hydrophobic
Positive charge
Negative charge
Polar
Cysteines
Glycines
Prolines
Aromatic

A

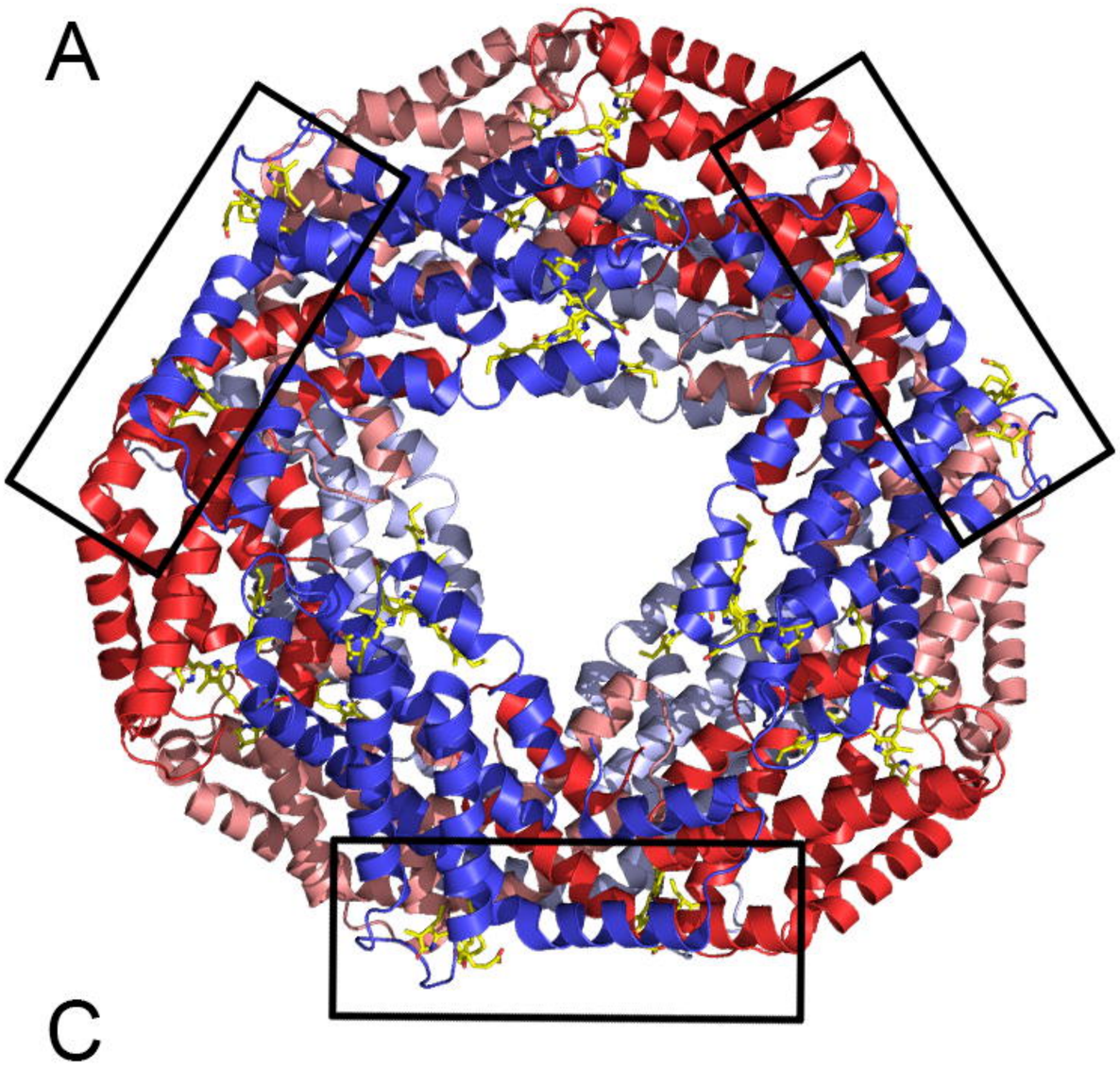

B

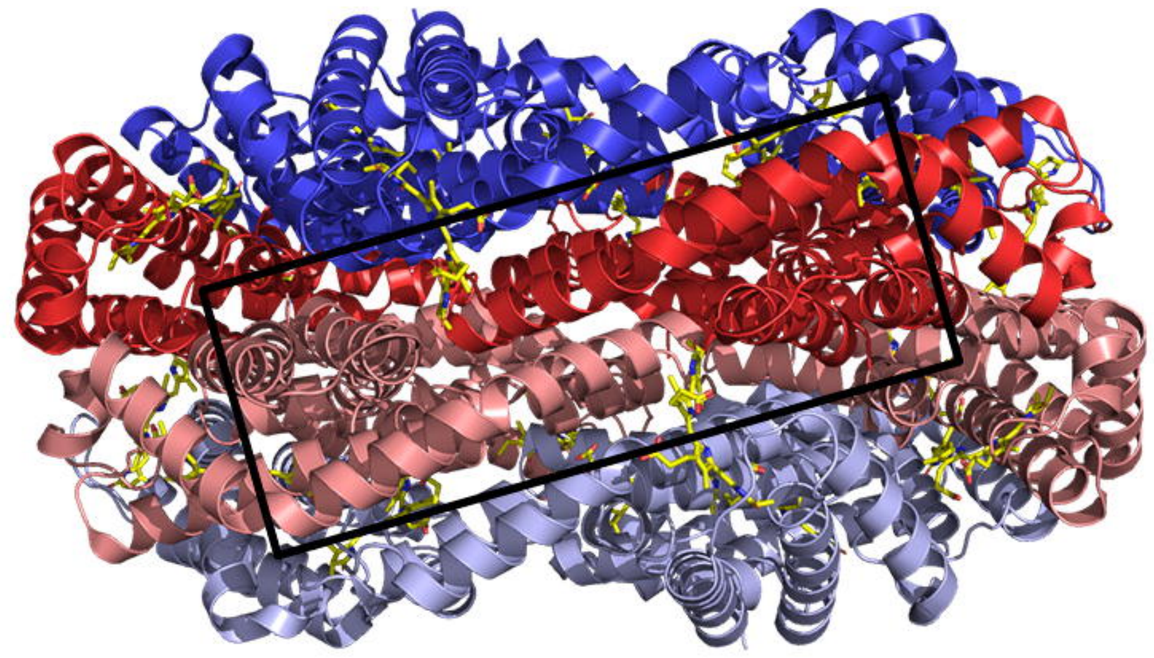

C

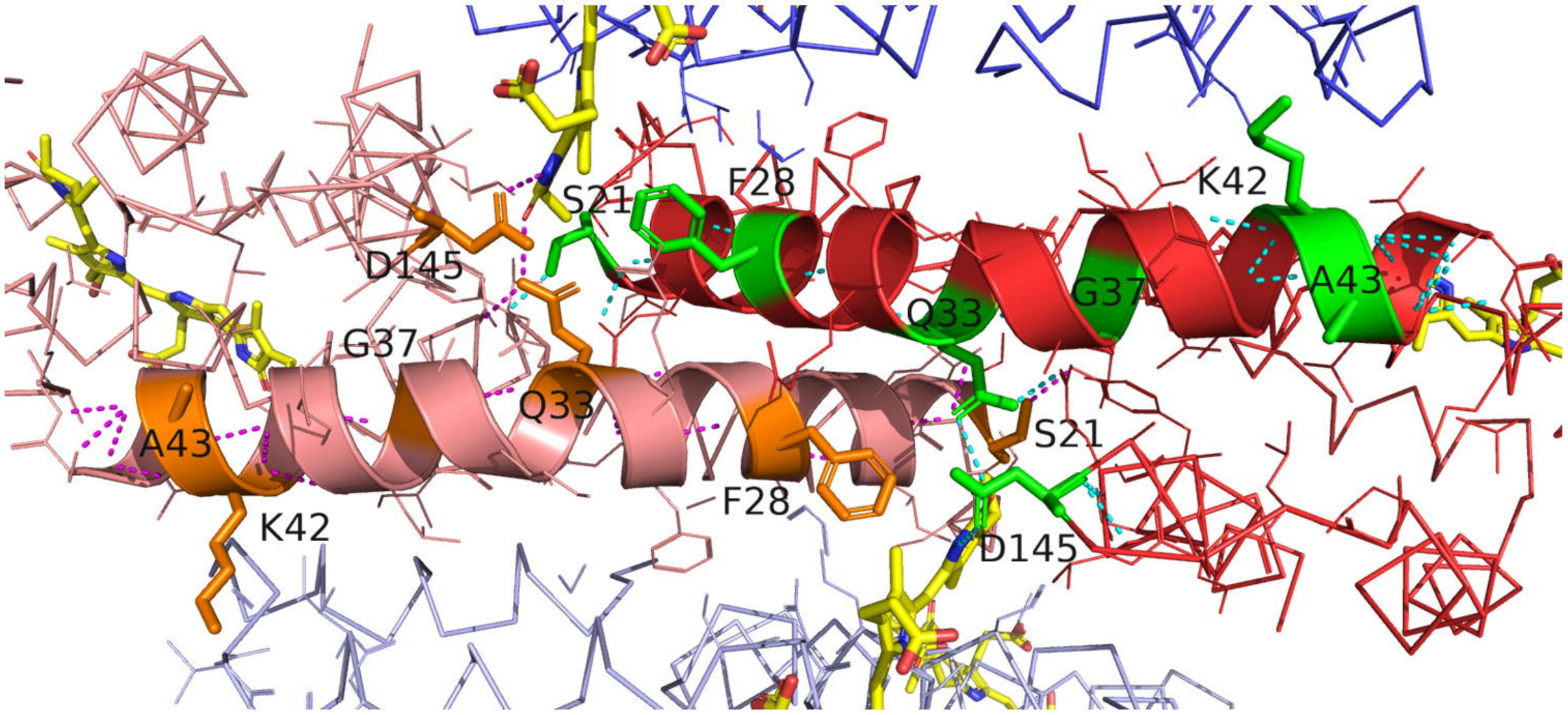
S21
F28
K42
D145
G37
Q33
A43
G37
A43
Q33
S21
K42
F28
D145

D

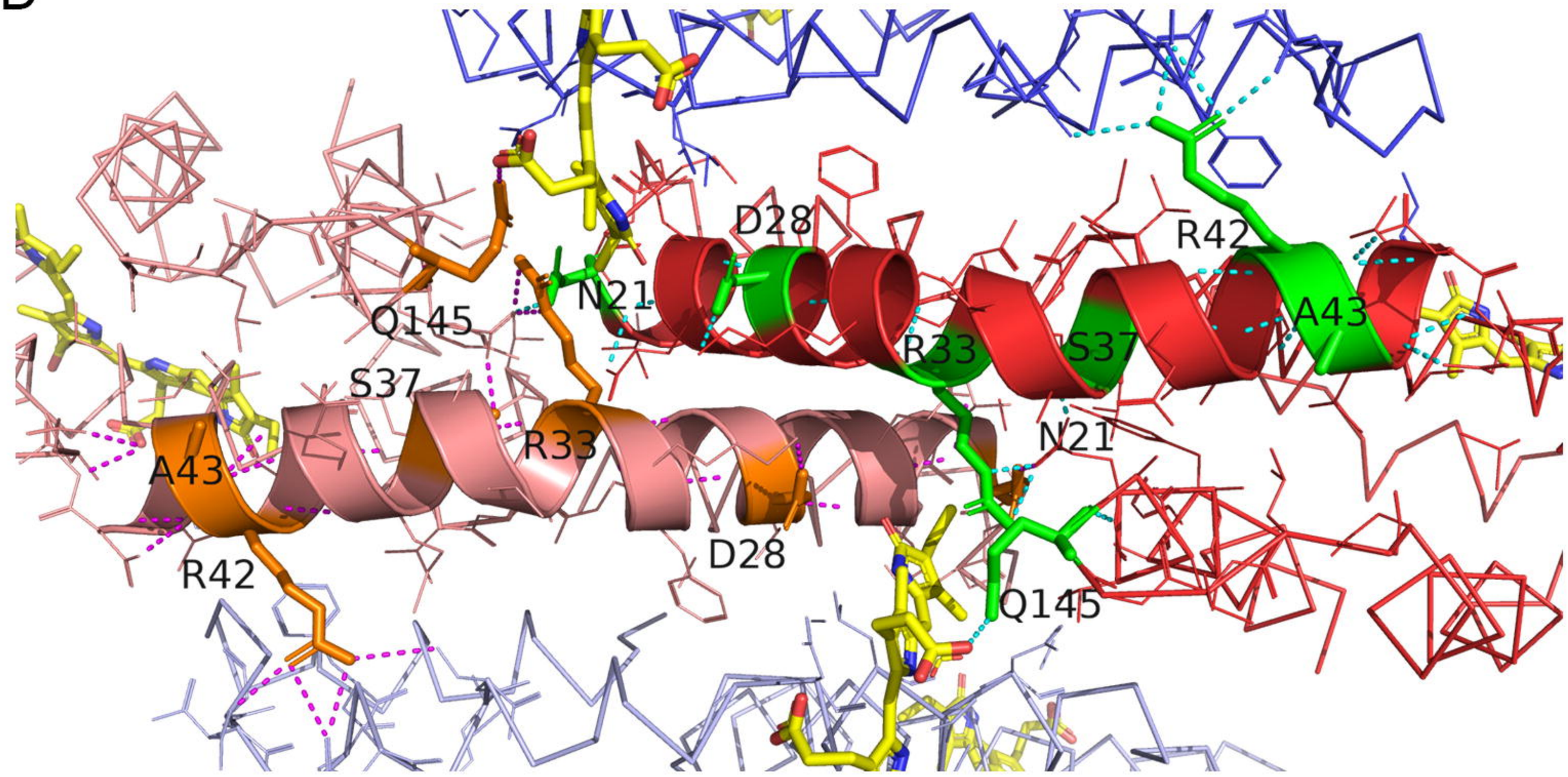
D28
R42
N21
Q145
S37
R33
S37
A43
A43
R33
N21
R42
D28
Q145